NOAA Atlas NESDIS 88

NORTHWEST ATLANTIC REGIONAL OCEAN CLIMATOLOGY version 2

National Centers for Environmental Information

Silver Spring, Maryland

November 15, 2022

U.S. DEPARTMENT OF COMMERCE

National Oceanic and Atmospheric Administration

National Environmental Satellite, Data, and Information Service

National Centers for Environmental Information

Additional copies of this publication, as well as information about NCEI data holdings and services, are available upon request directly from NCEI.

National Centers for Environmental Information
User Services Team
NOAA/NESDIS E/OC1
SSMC III, 4th floor
1315 East-West Highway
Silver Spring, MD 20910-3282

Telephone: (301) 713-3277
E-mail: NCEI.info@noaa.gov
NCEI URL: https://www.ncei.noaa.gov/

This document should be cited as:

Seidov, D., Mishonov, A.V., Baranova, O.K., Boyer, T.P., Nyadjro, E., Bouchard, C., Cross, S.L., 2022: *Northwest Atlantic Regional Ocean Climatology* version 2. NOAA Atlas NESDIS 88, Silver Spring, MD, 75 pp. doi: https://doi.org/10.25923/c6fz-fp67

This document is available at Northwest Atlantic Regional Climatology.

NOAA Atlas NESDIS 88

NORTHWEST ATLANTIC REGIONAL OCEAN CLIMATOLOGY version 2

Seidov, D., Mishonov, A.V., Baranova, O.K., Boyer, T.P., Nyadjro, E., Bouchard, C., Cross, S.L.

National Centers for Environmental Information

Silver Spring, Maryland

September 30, 2022

U.S. DEPARTMENT OF COMMERCE

Gina Raimondo, Secretary

National Oceanic and Atmospheric Administration

Dr. Richard Spinrad

Under Secretary of Commerce for Oceans and Atmosphere

National Environmental Satellite, Data, and Information Service

Dr. Stephen Volz, Assistant Administrator

This page intentionally left blank

TABLE OF CONTENTS

LIST OF FIGURES

Figure 10. Scheme used in computing annual, seasonal, and monthly objectively analyzed means for temperature and salinity (from Locarnini et al., 2018).

Figure 11. Winter objectively analyzed temperature averaged over the years 2005-2017 at 10 m depth in three analyses on: (a) one-degree, (b) quarter-degree, and (c) one-tenth-degree grids.

Figure 12. Winter objectively analyzed salinity averaged over the years 2005-2017 at 10 m depth in three analyses on: (a) one-degree, (b) quarter-degree, and (c) one-tenth-degree grids.

Figure 13. Winter statistical mean temperature averaged over the years 2005-2017 at 10 m depth in three analyses on: (a) one-degree, (b) quarter-degree, and (c) one-tenth-degree grids.

Figure 14. Winter statistical mean salinity averaged over the years 2005-2017 at 10 m depth in three analyses on: (a) one-degree, (b) quarter-degree, and (c) one-tenth-degree grids.

Figure 15. Standard error of temperature at 10 m depth for winter averaged over the period of 2005-2017 in three analyses on: (a) one-degree, (b) quarter-degree, and (c) one-tenth-degree grids.

Figure 16. Annual mean temperature at 10 m depth for three decades: (a) 1965-1974, (b) 1985-1994, and (c) 2005-2017 on one-tenth-degree grid.

Figure 17. Winter mean temperature at 10 m depth for three decades: (a) 1965-1974, (b) 1985-1994, and (c) 2005-2017 on one-tenth-degree grid.

Figure 18. January mean temperature at 10 m depth for three decades: (a) 1965-1974, (b) 1985-1994, and (c) 2005-2017 on one-tenth-degree grid.

Figure 19. March averages of SST for (left) 2003 and (right) 2007; SST fields are from the Remote Sensing Systems on a 0.258° grid (from Kelly *et al.* (2010).

Figure 20. Climatological October seawater temperature from (left) NWARC v1 at 10m depth on one-tenth-degree grid and (right) sea surface temperature (SST) from satellite observations for the decades 1985-1994, 1995-2004, and 2005-2012. The satellite SST maps are created from CoRTADv5 (Casey *et al.*, 2015). Examples of repetitive filaments in the GE Extension area are denoted by the black circles (reproduced from Seidov et al., 2018 with permission from American Meteorological Society).

Figure 21. January temperature at 10 m depth from (a) NWARC v1 and (b) the NEMO numerical experiments for the decade 1985-1994 (see the website NEMO ocean model).

Figure 22. July temperature at 10 m depth from (a) NWARC v1 and (b) the NEMO numerical experiments for the decade 1985-1994 (see the website NEMO ocean model).

LIST OF TABLES

ACKNOWLEDGMENTS

This work was completed by the Regional Ocean Climatology research team at the National Centers for Environmental Information (NCEI), formerly the National Oceanographic Data Center (NODC), in Silver Spring, Maryland, USA. The main purpose of the Regional Climatology Team is to prepare quality-controlled and objectively analyzed regional ocean climatologies in key regions of the World Ocean, and conduct preliminary diagnostic studies based on those climatologies. This publication presents the Northwest Atlantic (NWA) regional ocean climatology (NWARC) – the most recent and most advanced project in the series of regional climatology projects completed at NCEI to date. This regional climatology is an update of the first version NWARC, published in 2016 and is available at the NCEI website as NWARC version 2. For simplicity, further in the text, this update, NWARC version 2, is referred as NWARC v2, whereas the previous version is referred as NWARC v1.

The data on which this atlas is based are from the World Ocean Database 2018 and are freely distributed online by NCEI. Many data were acquired within the framework of the IOC/IODE Global Oceanographic Data Archaeology and Rescue (GODAR) Project, the IOC/IODE World Ocean Database (WOD) Project and World Data Center for Oceanography (WDC). At NCEI/WDC, data archaeology and rescue projects were supported with funding from the NOAA Environmental Science Data and Information Management (ESDIM) Program and the NOAA Climate and Global Change Program which has included support from both NASA and DOE.

We acknowledge the efforts and contributions by scientists, technicians, and programmers at NOAA and worldwide who have collected and processed data, those individuals who have submitted data to national and regional data centers, as well as the managers and staff at the various data centers. We are very grateful to our colleagues at the NCEI with whom we have had the privilege to work with for many years. Their efforts made this and all other works on regional climatologies possible. We are especially thankful for the lifetime effort of Sydney Levitus who pioneered and led the ocean climatology projects at NOAA for many years. We are very grateful to Kirsten Larsen and Rost Parson for their continuing support of the regional climatology projects at NCEI.

ABSTRACT

The Northwest Atlantic Ocean (NWA) plays a crucial role in global climate change. The Gulf Stream and North Atlantic Current System are the key elements of northward heat transport and the Meridional Overturning Circulation in the North Atlantic Ocean. The NWA includes a resource-rich coastal zone with abundant fisheries and other natural resources. Its economic significance and climatic importance resulted in many observational and research programs spanning many decades.

To provide an improved oceanographic foundation and reference for multidisciplinary studies of the NWA, the Regional Climatology Team at the National Centers for Environmental Information (NCEI), formerly the National Oceanographic Data Center (NODC) in Silver Spring, Maryland, USA, published the first version of the Northwest Atlantic Regional Climatology (NWARC v1) in 2016 (Seidov *et al.*, 2016). The NWARC v1 was based on the data from the World Ocean Database (WOD), referred as WOD13, published in 2013 (Boyer *et al.*, 2013). A new, updated version of the NWARC v2, now based on the most recent revision of the WOD (WOD18). It was developed and published by the NCEI Regional Climatology Team in 2021-2022 to provide a new set of high-resolution, quality-controlled, long-term annual, seasonal, and monthly mean temperature and salinity fields at different depth levels in the NWA region. This new version is based on the temperature and salinity profiles from oceanographic in situ observations spanning more than sixty years archived in the World Ocean Database up to 2018, adding five more years to the first edition of the NWARC. Note that updating WOD13 to WOD18 does not mean that only data collected from 2012 to 2017 were added; there were many historic data sets recovered from earlier cruises from 1955 to 2012 as well. That is, the updated WOD18 has new data in all six decades from 1955-1966 up to the last time interval of 2005-2017 (for simplicity, the time interval between 2005 and 2017 is referred to as a "decade" although it is three years longer than a regular decade).

When computing anomalies from a standard climatology (ocean climate obtained by averaging temperature and salinity fields over several decades), the mesoscale field is smoothed to prevent a generation of spurious anomalies. The smoothing depends on the spatial grid resolution and therefore can cause differences in computed climatological fields. On finer

resolution grids with lesser smoothing, climatological residual of mesoscale eddies with spatial scales longer than grid cell sizes can be directly resolved and the remaining mesoscale background presumably represents the cumulative effect of mesoscale dynamics rather than a noise caused by objective analysis. In this updated report, the theoretical background for the idea of eddy-resolving regional ocean climatology is briefly outlined based on the most recent peer-reviewed publications.

The advantages of high-resolution oceanographic data analysis stem from the use of short influence radii in the objective interpolation procedure leading to far less smoothing in the region of sharp frontal zones, especially in the coastal regions. In a sense, the finer-resolution analysis pursues the same goal as using progressively reduced grid sizes did in making headway from coarse-resolution to eddy-permitting and then to eddy-resolving numerical models of ocean circulation. The high-resolution regional climatologies are now closing the gaps existing between observations and model simulations thus allowing meaningful data-model comparisons in critical data-rich regions, such as the NWA.

1. INTRODUCTION

Over the past few decades, the earth's climate system has undergone profound and rapid changes. In the last one hundred years, climatologists and oceanographers invested great effort and resources in compiling reliable climatological products based on observations and developing new generations of ocean and climate models. Together, observations and modelling provide better understanding of the state and variability of the climate system, and better forecasting of the upcoming climate changes.

Understanding the coastal waters and their variability was critical for human activity and safety long before regular observations of the interior parts of the ocean basins, far from the shores, became viable. Moreover, the oceans and seas and their interaction with the atmosphere became a focal point of climate studies because of the ocean's role in the ongoing global warming (Blunden and Boyer, 2021; Zhongming *et al.*, 2021).

Over the past century, numerous intensive ocean observational programs provided a reasonably comprehensive assessment of the ocean climatic state and its long-term variability. In the North Atlantic, there were many dozens of studies that led to a very detailed view of this part of the World Ocean. Many national and international monitoring and research programs, including the International Ice Patrol (IIP) Survey, Ocean Weather Ships (OWS), Mid-Ocean Dynamics Experiment (MODE), US-USSR POLYMODE (Polygon and MODE), World Ocean Circulation Experiment (WOCE), Climate Variability and Predictability (CLIVAR) of the World Climate Research Programme (WCRP), Rapid Climate Change Programme (RAPID) and most recently Argo – to name just a few – contributed advanced understanding of North Atlantic climate dynamics; see a review in (Yashayaev *et al.*, 2015). In the 21st century, the ocean observations were immensely enhanced by the advent of Argo floats (Isachsen *et al.*, 2014; Johnson *et al.*, 2022; Riser *et al.*, 2016; Roemmich and Owens, 2002; Roemmich and Argo-Steering-Team, 2009; Steven *et al.*, 2017). The first Argo floats were deployed at the turn of the century, in 2000, and according to Johnson *et al.* (2022), after two decades, well over 2 million profiles were made publicly available in various databases including WOD18. Argo data have underpinned more than 4,000 scientific publications. Overall, the 'Argo Revolution' was met with great enthusiasm and immediate support by the ocean- and climate-research communities (Yashayaev *et al.*, 2015).

Argo floats were designed to overcome weather and other surface-state-related limitations to provide open-access, real-time and year-round profiles of temperature and salinity practically all over the World Ocean with a high degree of accuracy, e.g., (Gould *et al.*, 2004; Riser *et al.*, 2016; Toole *et al.*, 2011). To transmit data, Argo floats must reach the sea surface, although some researchers reported Argo floats with the ice-avoidance algorithm allowing the float to detect the presence of ice as they ascend (Klatt *et al.*, 2007). It was reported that such floats operated successfully in some ice-covered environments (Wong and Riser, 2011; 2013). Ice tethered profilers also promise to overcome the problems with under-ice observations (Toole *et al.*, 2011).

There have been a few Argo floats that reported from under-ice regions in the northern Labrador Sea included in NWA, but the more southern parts of NWA are rather densely covered by Argo profiler observations (e.g., see the map of Argo coverage in (Riser *et al.*, 2016). Although Argo data provides coverage away from the shelf zone and ice-covered regions, they are an important new tool for studying the open ocean in the NWA region, even if the addition of Argo data is not as substantial there compared to more remote regions, for example in the Southern Ocean. To further boost the use of this new oceanographic instrumentation, a new expansion of the Argo program — the OneArgo program — is on the way (Owens *et al.*, 2022). Within this new program, it is expected that the upper ocean measurements will be extended to high latitudes and marginal seas, the deep ocean measurements will be expanded over the large part of the ocean areas below 2,000-m depth, and many biochemical parameters will be additionally measured, e.g., dissolved oxygen, pH, nitrate, chlorophyll, etc.

Ocean gliders are another modern autonomous maritime data acquisition technology (Meyer, 2016; Rudnick, 2016), which rapidly increases high-resolution data inflow especially in the shelf areas (Mesick *et al.*, 2020). Major source of the glider data in WOD for the NWA area is IOOS-NGDAC (https://ioos.noaa.gov/), which collect glider data from Federally owned observing systems and non-federal data providers, develops, integrates, and submits these data to the NCEI archives.

The climate is formally defined as the ensemble of states that the major components of the planetary climate system – ocean, atmosphere, cryosphere, biosphere, landmass, and its waters – transit through within a certain period, most often defined as thirty years (Monin, 1986; WMO, 2011). This time interval complies with the World Meteorological Organization (WMO) general

recommendation of using 30-year periods of reference. According to this definition and because the time scale of the ocean processes is much longer than those of the atmosphere, the ocean is the key element of the climate system on decadal to centennial time scales. Therefore, the knowledge of the decadal changes of ocean parameters, especially temperature and salinity, is crucial for understanding and predicting climate variability on those time scales comparable to the average span of a human generation.

A fundamental concept used in climatology is the concept of "climate normals" serving as a benchmark for which recent or current observations can be compared. Practically speaking, the normals are averaged climate system parameters (temperature, salinity, pressure, etc.) within selected intervals (months, seasons, and years) over the reference 30-year periods. IMO/WMO member nations were first mandated to compute climate normals for their member countries for the 1901–30 period and are required to update these climate normals every 30 years, resulting in the 1931–60 normals and the 1961–90 normals (Arguez and Vose, 2011).

Since 1956, the WMO has recommended that each member country re-compute their 30-year climate normals every 10 years. Thus, currently the 1991-2020 is the preferred 30-year interval for computing climate normals, and the new ocean climate normals for this interval expected to be published by NCEI in 2022. It should be mentioned that justifications for using 30-year normals for describing climate are now being questioned (Guttman, 1989; Livezey *et al.*, 2007) and implying that a longer time interval should be used as a reference mean to compute anomalies. Therefore, in ocean heat content calculations, first published in (Levitus *et al.*, 2000), and then updated in 2009 and in 2012 (Levitus *et al.*, 2009; Levitus *et al.*, 2012) the reference mean or base climatology was set to the entire period from 1955 to 2006, which is 50 years, i.e., much longer than the WMO-recommended 30 years, to reflect the prolonged time of thermocline water turnover (Levitus *et al.*, 2009). Currently this longer time interval is used in the routine computation of ocean heat and salt content anomalies regularly updated at the NCEI Global Ocean Heat and Salt Content web site: NCEI Global Ocean Heat and Salt Content. This will change when the new ocean climate normals for 1991-2020 become available.

The time scales of the ocean circulation, which are the key to the ocean's role in the earth climate dynamics on millennial and shorter time scales, are very different in the upper ocean, in the main thermocline, and in the deep ocean. They can also vary from years at a basin scale to

hundreds of years at the global scale. The longest time scales of several centuries are determined by the global thermohaline circulation or inter-basin exchange of thermocline water (Gordon, 1986), also known as a "global conveyor" (Broecker, 1991). However, a practical approach to ocean climate diagnostics is the use of data obtained in the last sixty plus years following the advent of widespread and numerous ocean observations in the middle of the twentieth century.

There is a strong consensus among climate scientists that the main climate controls imposed on the earth's climate system by the oceans are via air-sea heat and freshwater exchange. The oceans gain heat in the tropics and sub-tropics and release it in high latitudes. The meridional overturning circulation that regulates the poleward heat transport by ocean currents facilitates redistribution of energy between the low and high latitudes in the oceans and eventually, via air-sea interactions, in the climate system. The thermohaline structure of the World Ocean reflects all three factors – ocean-air heat exchange (controls surface water temperature), evaporation-precipitation balance (paired with melting and freezing of sea ice and river runoff, controls surface water salinity), and advection of heat and salt in the ocean-by-ocean currents.

As ocean currents are driven by wind and density gradients, there are feedbacks, both in the ocean and atmosphere controlling the ocean-atmosphere interactions and ultimately the Earth's long-term climate state and variability. To understand and forecast ocean conditions and future changes, there is a need for ocean observations that are quality controlled and readily available to support all kinds of ocean-related research. Two main tools answering this call – the World Ocean Database (WOD) and the World Ocean Atlas (WOA) – were developed at NCEI.

2. WORLD OCEAN DATABASE

The entire Earth climate dynamics and its long-term variability can be properly diagnosed only if the ocean changes can be assessed on the time scale of at least several decades. Therefore, the ocean-driven climate paradigm calls for developing oceanographic databases of quality-controlled historic ocean data to reveal ocean thermohaline variability on decadal and longer time scales. One of the largest and most advanced world ocean databases is the WOD compiled at NCEI (formerly NODC) in Silver Spring, Maryland, USA. The first edition of the WOD was developed at NODC in 1994 and has been updated regularly since then. The updates include WOD98,

WOD01, WOD05, WOD09, WOD13, and WOD18 (two last digits indicates the year of revision release).

The WOD contains several essential oceanic parameters, such as temperature, salinity, oxygen, nutrients, etc. The fundamental element of the WOD is a profile (used to be called "cast' for onboard instrument deployments). A profile is defined as a set of measurements for a single variable (temperature, salinity, etc.) at discrete depths taken as an instrument drops or rises vertically in the water column (Boyer *et al.*, 2018a).

The hydrographic profiles in WOD are from in situ observations collected with various oceanographic instruments. Historical oceanographic temperature and salinity data from bottle samples or "Ocean Station Data" (OSD), Mechanical Bathy-thermographs (MBT; measuring only water temperature), ship-deployed Conductivity-Temperature-Depth (CTD) packages, Digital Bathythermograph (DBT; measuring only water temperature), Expendable Bathythermographs (XBT; measuring only water temperature), profiling floats (PFL), moored (MRB) and drifting (DRB) buoys, gliders (GLD), and undulating oceanographic recorders (UOR) profiles used in all World Ocean and regional climatology projects were obtained from the NCEI/NODC/WDC archives (WDC stands for World Ocean Center for Oceanography) and include all data gathered as a result of the GODAR and WOD Projects.

For climate studies, as well as for much ecosystem research, the key oceanographic values are temperature and salinity. WOD is the quintessential tool for assessing the long-term multi-decadal ocean climate variability in many regions of the World Ocean. The most up-to-date release of this database, WOD18, allows computing statistics and analyses through the end of 2017. The online version of the WOD, which is being updated quarterly contains over 17.8 million temperature and over 10.5 million salinity profiles. It is available at the NCEI's World Ocean Database web site (Boyer *et al.*, 2018a).

Temperature and salinity profiles are available for download in a uniform format with associated metadata and quality control flags. With such abundant temperature and salinity data, WOD18 has become even more invaluable for characterizing ocean climate states and trend at many locations and for various time intervals. However, in many applications, there is a strong demand for analyzed rather than raw data sets available through WOD.

3. WORLD OCEAN CLIMATOLOGY

The idea of calculating and mapping the long-term ocean state using all available historic oceanographic observations was first executed by Sydney Levitus at NOAA. Recorded oceanographic observations in the world's oceans and seas have more than 300 years of history, yet the first detailed global ocean water properties maps were compiled and published in the Climatological Atlas of the World Ocean in 1982, just about forty years ago (Levitus, 1982). That first edition of this Atlas, known under the name of World Ocean Atlas (WOA) in all subsequent editions, was comprised of temperature, salinity, oxygen, and nutrients interpolated to a regular one-degree geographical grid at 33 standard depth levels from the surface to 5500 meters (Table 3, bold numbers). The monthly, seasonally, and annually averaged values of those parameters over the time of several decades were called "ocean climatologies" and used as the descriptors of the climatic state (i.e., averaged over many decades) of the ocean in numerous applications thereafter.

Although WOA has become a tool of choice for many scientific groups and individuals, the community of ocean, climate and earth system modelers is perhaps one of the premier groups of users of the ocean observed climatology. At the time when the Climatological Atlas of the World Ocean was published (Levitus, 1982), two-to-one-degree spatial resolution was the limit that could be achieved with then existing computing power and availability of data (Cox, 1975; Semtner and Chervin, 1988). In the 80s and beginning of 90s, there was a close match between the so-called non-eddy-permitting and early eddy-permitting models with sub-one-degree resolution and the WOA (there is a difference between "eddy-permitting" and "eddy-resolving" models, with the latter requiring at least one-tenth of a degree resolution; see below in this section). For example, Semtner and Chervin (1988) constrained the computed thermohaline fields between 25 m and sea surface and below 700 m in a global eddy-permitting model with half-degree resolution by restoring them to the gridded data from Climatological Atlas of the World Ocean (Levitus, 1982). It was soon found, however, that some elements of the modeled ocean climate cannot be properly resolved in ocean computer simulations with grid resolution coarser than a certain limit specific to those elements. For example, it was found that the spatial grid resolution sufficient for proper simulation of the Gulf Stream dynamics should be one-sixth of a degree or better (Chao *et al.*, 1996).

What was technically impossible only about 30 years ago, had become feasible in late '90-s following a rapid surge in computing power and improved modeling skills (Maltrud and McClean, 2005; Semtner and Chervin, 1993; Semtner, 1995). By resolving ever-shorter spatial scale processes in the ocean, climate models have greatly surpassed the one-degree WOA resolution in providing far more detailed ocean simulated climatologies. Employing finer and finer resolutions in ocean and climate models continues with an increasing pace toward fully resolved mesoscale and even shorter spatio-temporal scales of ocean and climate dynamics.

Ocean models now fall in one of three major categories—the coarse-resolution or non-eddy-permitting, eddy-permitting, and eddy-resolving (Barrier *et al.*, 2015; Marzocchi *et al.*, 2015; Nakamura and Kagimoto, 2006). The eddy-resolving ocean models with one-tenths and/or one-twelfth degree grids are quickly replacing the eddy-permitting ocean models with horizontal grid sizes between half- to quarter-degree resolution (Barrier *et al.*, 2015; Bernard *et al.*, 2006); see a review in (Hurlburt *et al.*, 2008). Coarse-resolution ocean models are quickly becoming obsolete and are used mostly in qualitative rather than quantitative ocean climate simulations.

To narrow the gap between observed and modeled ocean climatologies and to better serve the oceanographic community who rely on the NODC/NCEI ocean climatology products, quarter-degree temperature and salinity fields were first compiled by (Boyer *et al.*, 2005) at 33 depth levels. At the next step, a new edition - World Ocean Atlas 2018 (WOA18), which is the most recent descendant from the original Climatological Atlas of the World Ocean, was compiled at 1/4°x1/4°-degree resolution at 102 depth levels for six decades World Ocean Atlas 2018. With a large number of new profiles added to WOD, this edition of WOA is far more detailed than all previous releases since 1982 (Boyer *et al.*, 2018b). NCEI regional climatologies are now extending this effort to provide one-tenth of a degree resolution in several critical ocean regions.

All new regional climatologies are structured very similarly to the WOA. Compilation and analyses of regional climatology inherit all WOA techniques and methodology.

As was mentioned above, the new class of eddy-resolving ocean models that are capable of properly resolving the mesoscale eddies and their interactions with large-scale currents are now taking the stage and will soon become a major requirement of any realistic climate forecast system. To comply with modern modeling development pace, the observed climatologies must break through the quarter-degree spatial resolution barrier and settle at one-tenth-degree or better. The

main obstacle in attaining such resolutions is the lack of adequate data coverage in most parts of the World Ocean except for a few, albeit critically important, regions. To generate high-quality regional climatologies with as high spatial resolution as possible in regions that have sufficient data coverage, the NCEI Regional Climatology project was introduced in 2011 and is described in the following section.

4. NCEI REGIONAL OCEAN CLIMATOLOGY PROJECTS

With modern computing facilities, it would be relatively easy to generate an ocean climatology on grids with very fine resolution. However, in contrast with numerical models, the grid resolution in observed ocean climatologies is restricted not by computer power, but by availability of field data. The above-mentioned eddy-resolving ocean models can generate high-resolution output uniformly on any chosen grid anywhere, even over the entire World Ocean, but a high spatial resolution ocean climatology is supported by observations only in a limited number of regions of the World Ocean. Therefore, a global "high resolution" ocean climatology would be such in the name only. Indeed, many grid cells in WOA18 contain less than three observed values on the quarter-degree grid (see data distribution maps at World Ocean Atlas 2018).

In contrast to the most parts of the World Ocean, there are a few regions where data availability may support true high-resolution ocean climatologies. A new level of detail is therefore achievable, even if only regionally. Coincidentally but not surprisingly, all those regions are critically important for climate science, fishery, navigation, etc. Therefore, far more attention was directed toward better oceanographic description of those areas where humans most needed such a description.

The first regional climatology project had emerged and matured as a response to the urgent oceanographic research efforts linked to the Deepwater Horizon Oil Spill disaster in the Gulf of Mexico in April 2010. As a part of a wider multi-institutional project of compiling a new electronic edition of the NOAA Gulf of Mexico Data Atlas, a team of collaborators at NCEI (then NODC), created the Gulf of Mexico (GOM) Regional Climatology with one-quarter and one-tenth degree resolutions. After this first implementation, other projects followed: the Oceanographic Atlas of the East Asian Seas (EAS), the Arctic Regional Climatology (ARC), the Greenland-Iceland-Norwegian Seas (GINS) Regional Climatology, Northwest Atlantic (NWA), Northern North

Pacific (NNP), Northeastern Pacific (NEP), Southwest North Atlantic (SWNA), and, most recently, GOM Regional Climatology version 2. All completed to date regional climatologies published at the NCEI regional ocean climatologies web portal are shown in Figure 1.

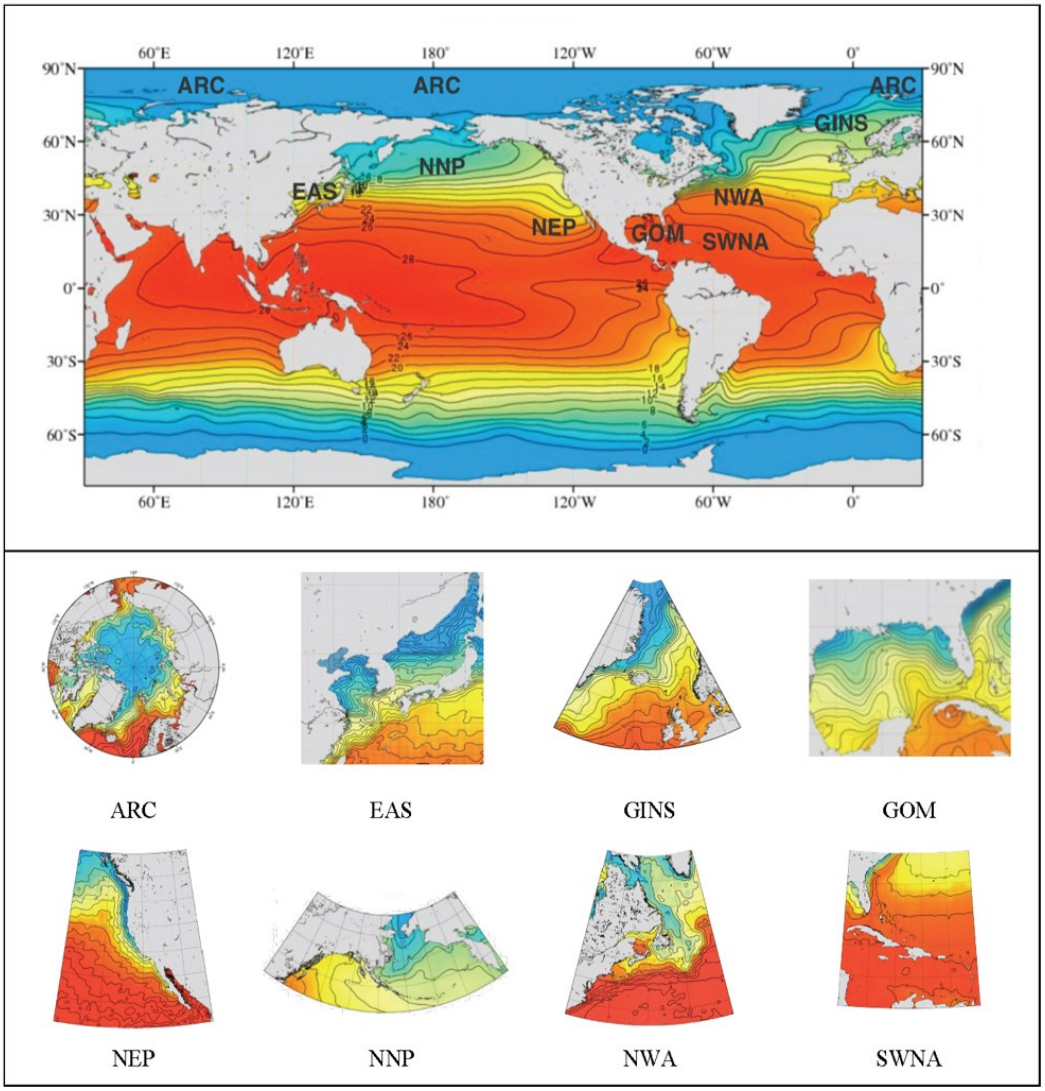

Figure 1. NCEI regional climatologies completed to date. The background map for the regional climatologies is the sea surface temperature map from World Ocean Atlas (WOA18). The abbreviations of the regional climatology names are (alphabetically): ARC— Arctic, EAS—East Asian Seas, GINS—Greenland, Iceland, and Norwegian Seas; GOM—Gulf of Mexico version 2; NEP—Northeast Pacific; NNP—Northern North Pacific; NWA—Northwest Atlantic, and SWNA—Southwest North Atlantic.

The locations of the regional climatologies are marked on the World Ocean surface temperature map from WOA18, and the individual regional climatologies are listed below the map (in alphabetical order).

The key difference between regional versus global climatology approach is that observed data in the few selected regions have far fewer spatial and temporal data gaps to be filled by interpolation than almost anywhere else in the World Ocean. Importantly, quality control on a finer spatial resolution grid reveals more obvious outliers than on coarser resolution grids. One of the advantages of compiling regional ocean climatologies is more elaborate quality control of data made on higher resolution grids. It in turn is instrumental for improving WOD and recursively WOA quality by providing additional feedback in the areas of regional climatologies because of the quality control on a finer grid. Yet the most important advantage of regional climatologies is the dense spatial distribution of oceanographic measurements, helping to retain the sharpness of frontal zones and resolving many cumulative mesoscale features (quasi-stationary local vortices, topographic meanders, etc.; see the discussion in Chapters 9 and 10). In the next section, the advanced features of regional climatologies will be demonstrated using the maps on one, quarter, and one-tenths of a degree grids for the newest and most up to date advanced regional climatology, the NWARC v2.

5. NORTHWEST ATLANTIC OCEAN CLIMATE OVERVIEW

Selecting a region for compiling a regional climatology is not a trivial task. Firstly, the region should be of high importance for several Earth System science disciplines (e.g., oceanography, climatology, ecology, etc.), as well as for applications and allied sciences, such as fisheries, coastal engineering, coastal economics, etc. Secondly, the goal of compiling a reliable high-resolution climatology must be achievable, i.e., the density of oceanographic observations must be sufficient for such high-resolution compilation. The Northwest Atlantic is an exemplary region where the research and practical demands imposed on the needed oceanographic data are supported by data coverage. To understand why this region was selected for detailed analysis on as fine of a grid as possible based on data coverage, and to justify the NWARC v2 project in general, some insights into major characteristics of the NWA dynamics and its climate role are outlined briefly in this and the next sections.

As an element of Earth's climate system, the Gulf Stream is perhaps the most important ocean current system in the World Ocean. The Gulf Stream originates as the Florida Current and flows along the U.S. East Coast to Cape Hatteras, where it separates from the coast and becomes

the North Atlantic Current. Many features of the Gulf Stream System are determined by the bottom topography and the structure of the shelf break of the western North Atlantic Ocean. The Gulf Stream System occupies the western part of the basin, as shown in Figure 2.

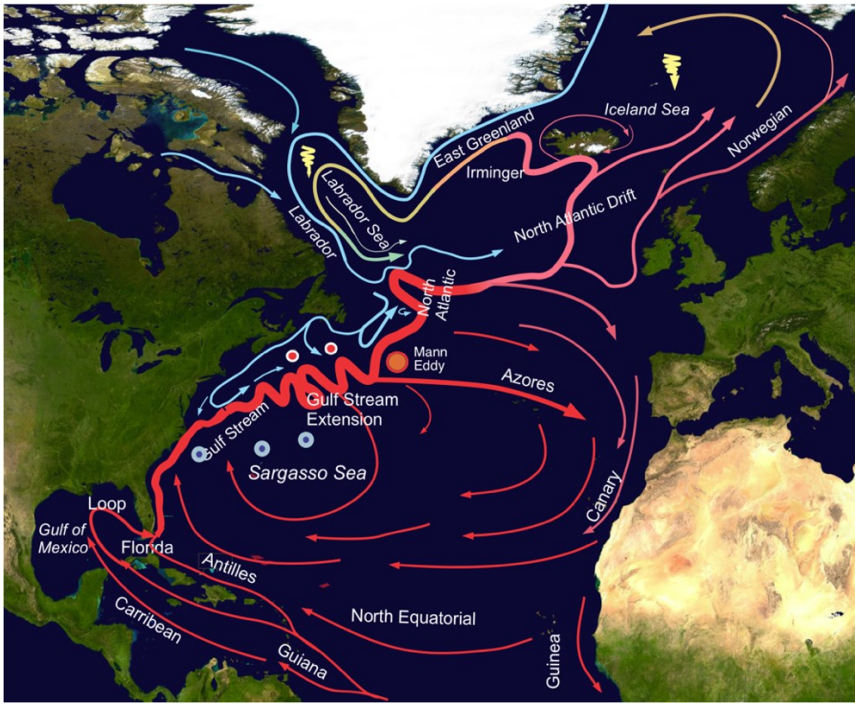

Figure 2. Scheme of the Northwest Atlantic Current System (modified from Seidov et al., 2018; initial courtesy of I. Yashayaev). Red lines show warm and blue lines show cold currents; the convection sites in the Labrador and Greenland seas are depicted as yellow downward spirals; warm and cold Gulf Stream rings are shown as small orange and blue circles north and south of the Gulf Stream and its extension.

Along the U.S. East Coast, the Gulf Stream is strengthened by the northern branch of the North Equatorial Current; the warm southern Gulf Stream recirculation gyre; and the cold northern recirculation gyre. In the north, the North Atlantic Current collides with the Labrador Current to form the Mid-Latitude Transition Zone (MLTZ) east of Newfoundland and the Great Banks. The Gulf Stream System, the Labrador Sea currents, the North Atlantic Current, and the MLTZ comprise four main elements of the NWA ocean current system (Figure 2).

The Gulf Stream Current System is perhaps one of the most studied and charted ocean current systems to date. By the mid-20th century, oceanographers had already gained rather detailed knowledge of the Gulf Stream, especially in close vicinity to the U.S. East coast (Fuglister, 1963; Iselin, 1936; Iselin and Fuglister, 1948; Stommel, 1958). Just north of Florida Strait, there is a confluence of the Florida Current and the eastbound parts of the Caribbean and Antilles currents

– two derivatives of the westbound North Equatorial Current as it reaches the Antilles Islands –the southwest-most part of the large anticyclonic subtropical ocean circulation gyre generated by the anticyclonic wind stress curl over the subtropical North Atlantic. The westward intensification of the Gulf Stream as a western boundary current is caused by the Coriolis Effect on the spherical Earth (Hogg and Johns, 1995; Munk, 1950; Stommel, 1948; 1958). The jet further intensifies between Florida Strait and Cape Hatteras by the entrainment of the water from two inner recirculation gyres to the north and south of the Gulf Stream core. The position of the stream as it leaves the coast changes throughout the year. In the fall, the core of the Gulf Stream shifts to the north, while in the spring it shifts to the south (Hogg and Johns, 1995; Schmitz and McCartney, 1993).

The two upper-ocean recirculation gyres mentioned above are the cold and warm gyres north and south of the eastbound Gulf Stream core. The cold water from the Labrador Sea flows westward along the coast (this flow is also known as the Slope Water Current). The warm water south and east of the Gulf Stream and its continuation circulates around the Sargasso Sea and comprises the Gulf Stream Recirculation Gyre (Hogg *et al.*, 1986; Worthington, 1976), also known as the Worthington Gyre, between 55ºW and 75°W (Hogg *et al.*, 1986). Both currents feed the eastbound stream and contribute to the Gulf Stream transport increase between the Florida Strait and Cape Hatteras and especially further on along the Gulf Stream Extension.

After breaking from the continental shelf, the eastbound Gulf Stream becomes the Gulf Stream Extension and continues to strengthen before it turns north at the eastern flank of the Great Banks and finally becomes the North Atlantic Current (Hogg and Johns, 1995; Wunsch, 1978). The Gulf Stream Extension is a free baroclinic jet penetrating to the ocean bottom and its structure changes from a single, meandering front to multiple, branching fronts with a great deal of mesoscale activity and increasingly large meanders. By 65°W the meandering envelope is nearly 500 km wide, which is five times the jet width at the separation point near Cape Hatteras. The water transport almost doubles downstream between Cape Hatteras and approximately 55°W resulting from the water fed by the Northern Recirculation Gyre (the Slope Water Current) and the Worthington Gyre.

The meanders and mesoscale eddies west of the North Atlantic Current comprise the MLTZ (see above) where cold and relatively fresh eastward flowing water from the Labrador Sea

mixes with the warm and salty north-northeast flowing water of the Gulf Stream and North Atlantic Current (see Figure 3 above). Thus, the Gulf Stream, being a highly stratified (both vertically and horizontally) and very unstable jet current, serves both as a barrier and a blender of warm and cold waters along its edges. Blending, or mixing, of those waters is enabled by meanders and mesoscale eddies (Bower *et al.*, 1985). Further mixing is done by the so-called sub-mesoscale streamers that transition between eddy-induced mesoscale geostrophic mixing and smaller-scale turbulent mixing. New research shows that this type of mixing is especially important at the Cold Wall of the Gulf Stream, where the outer warm core of the Gulf Stream contacts the cold water that originated in the Labrador Sea (Gula *et al.*, 2014; Klymak *et al.*, 2016) (see also Figure 3).

There are two types of meanders: those generated by internal dynamic instability like in a free turbulent flow, and the quasi-stationary ones caused mostly by bottom topography. The large-amplitude meanders occasionally break off from the jet to form warm- and cold-core Gulf Stream rings (Figure 2). Anticyclonic warm core rings are found north of, and cyclonic cold core rings are found south of the Gulf Stream core. The rings migrate westward and occasionally remerge with the Gulf Stream.

The rings and meanders facilitate effective heat and salt exchange across the Gulf Stream frontal zone. Another source of mesoscale activity that can cause large-scale variability on longer time and space scales are the mesoscale eddies that are also known as geostrophic turbulence (Kamenkovich *et al.*, 1986; Rhines, 1979) analogous to atmospheric eddy-like motion (Charney, 1971). Nonlinear eddies are important mixing agents of the large-scale ocean circulation capable of rather efficient transport of water parcels and their associated physical, chemical, and biological properties across strong frontal zones (e.g., (Bower *et al.*, 1985; Bryan, 1986; Chelton *et al.*, 2011; Rhines, 2001). In general, the kinetic energy of mesoscale eddies surrounding strong jet-like currents is larger than the kinetic energy of the averaged mean flow. Those eddies are also thought to generate upscale energy flow to intensify large-scale currents (Chao *et al.*, 1996; Kamenkovich *et al.*, 1986; Seidov, 1989; Seidov and Maruskevich, 1992). The thermohaline structure of the Gulf Stream reflects eddy-jet dynamics (Richardson, 2001). Snapshots of sea surface temperature in the Gulf Stream region using satellite imagery or eddy-resolving models show very intense mixing and turbulent structure with clearly seen mesoscale eddies, meanders, and rings, as shown in Figure 3.

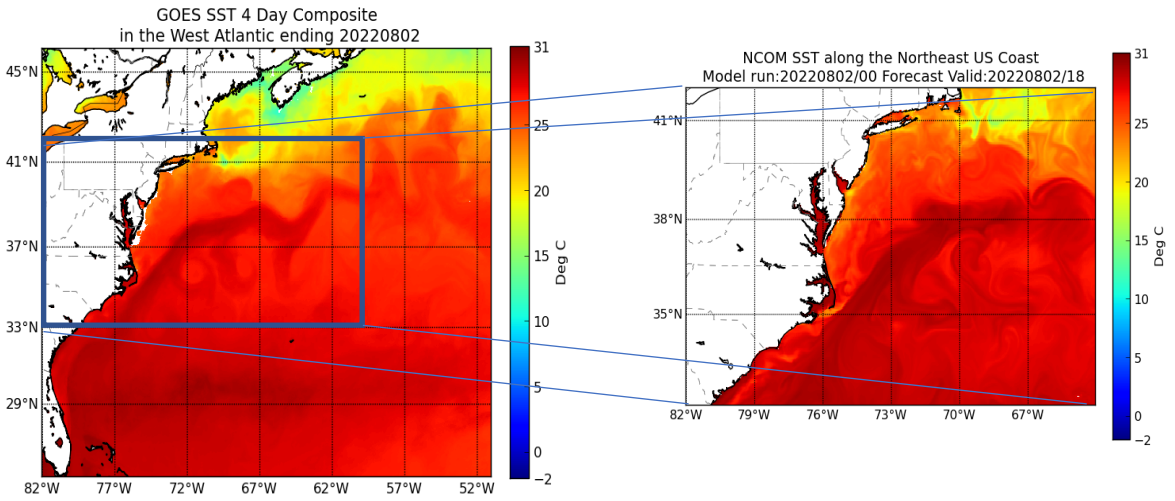

Figure 3. Snapshot of observed and modelled sea surface temperature in the Gulf Stream region: (left) from GEOS satellite-derived sea surface temperature record, and (right) from US Navy NCOM High Resolution Ocean Model (source: NOAA Ocean Prediction Center NCOM High-resolution Ocean Model).

As mentioned before, the east-northbound Gulf Stream along the North America east coast and the Gulf Stream Extension are energetic baroclinic currents with a strongly stratified warm and salty core shoaling downstream. In contrast, the east-southbound Labrador Current is much more barotropic with both upper and lower branches flowing south-east along the Canada and U.S. eastern shelf and continental slope, known also as the Western Boundary Current or WBC (upper branch) and Deep Western Boundary Current or DWBC (deep-sea branch) of the Labrador Sea. The DWBC is the deep limb of the Atlantic Meridional Overturning Circulation—one of the key elements of global ocean circulation and one of the most important oceanic climate controls.

6. ATLANTIC MERIDIONAL OVERTURNING CIRCULATION

One of the major goals of NCEI global ocean and regional climatologies is to support ocean climate research, especially the exploration of global and regional ocean thermohaline circulation shaping the earth's global climate and thus being a focus of modern climate studies. The NWARC v2 is specifically targeting a region fundamentally important for the entire climate system. Indeed, of all branches of the global thermohaline circulation (Gordon, 1986), also known as a "global conveyor belt" (Broecker, 1991), the most important is the Atlantic branch usually referred to as the Atlantic Meridional Overturning Circulation (AMOC). The AMOC is thought to be the most important driver of ocean climate variability on decadal and longer time scales (Bower *et al.*, 2019;

Bryden *et al.*, 2005; Buckley and Marshall, 2016; Dai *et al.*, 2005; Frajka-Williams *et al.*, 2019; Lozier *et al.*, 2017; Mahajan *et al.*, 2011; Srokosz *et al.*, 2012).

The AMOC's near-surface, warm northward flow is compensated by a colder southward return flow at depth. The AMOC carries warm water to high latitudes where heat loss to the atmosphere leads to the formation of the North Atlantic Deep Water (NADW) in the northern North Atlantic, Nordic and Labrador Seas. The deep southward flow of NADW comprises the deep branch of the AMOC. The strength of the AMOC and meridional heat transport are estimated as 17.2 Sv and 1.25 PW (1 Sv=10^6 m^3s^{-1}; 1 PW=10^{15} W) (McCarthy *et al.*, 2015); maximum transport was recorded as high as 18.7 Sv (Rayner *et al.*, 2011).

Changes in the AMOC can contribute to climate changes on regional and even global scales in ways that are yet to be completely understood. On interannual to decadal timescales, AMOC changes are primarily caused by buoyancy anomalies on the western boundary and in the MLTZ (see above), or a "western transition zone" between the subtropical and subpolar gyres (Buckley and Marshall, 2016). A decline in AMOC transport over the past couple of decades has been reported in a number of publications (Bryden *et al.*, 2005; Caesar *et al.*, 2018; Cunningham *et al.*, 2007; Smeed *et al.*, 2014; Smeed *et al.*, 2018), although some authors believe that there was no slowdown of the Gulf Stream seen in observations on a longer time scale (Rossby *et al.*, 2010; Rossby *et al.*, 2014; Worthington *et al.*, 2021); see a recent review in (Jackson *et al.*, 2022). It is instrumental to see if the interannual and decadal variability of the AMOC is manifested clearly in historical oceanographic data, or, alternatively, how the AMOC long-term variability connects to ocean changes revealed in the in situ decadal-scale oceanographic observations integrated in WOA18 and NWARC v2.

One of the important questions linked to AMOC functionality is about the large temperature and salinity anomalies in the Gulf Stream area due to the jet wobbling and path shifts. The Gulf Stream path shift attracted much attention over the years, e.g., (Cornillon and Watts, 1987; Joyce and Zhang, 2010; Lee and Cornillon, 1995; Peña-Molino and Joyce, 2008; Seidov *et al.*, 2019b; Taylor, 1996; Taylor and Stephens, 1998). Many factors could influence the Gulf Stream path shifts if such a shift had indeed occurred on the decadal time scale. The high-resolution NWARC v2 could be used to verify whether decadal shifts of the thermal front can be diagnosed from historic hydrographic data. As the jet width itself is on the order of ten to a hundred

kilometers, the minimum latitude-longitude resolution that is sufficient to pursuing this goal is 0.1°x0.1° or better. Thus, this is another obvious motivation for compiling a high-resolution climatology in this region. In fact, the Gulf Stream path shift is clearly seen in an earlier high-resolution NWARC v1 analysis (Seidov *et al.*, 2019a) and has been studied in detail using in situ data. It has been shown that the Gulf Stream axis migration caused by the overall warming trend in the Gulf Stream surrounding is quite substantial, especially in the last decade, e.g., (Seidov *et al.*, 2017; 2019b; Seidov *et al.*, 2021)

7. NORTHWEST ATLANTIC OCEAN CLIMATE AND ECOSYSTEM DYNAMICS

The NWA is a resource-rich coastal zone with abundant fisheries and other substantial natural resources. Its economic significance and climatic importance spurred intensive observational and research programs spanning many decades. Climate change has always affected fisheries, e.g., (Lehodey *et al.*, 2006), but the North Atlantic fisheries dependence on the long-term ocean climate variability was especially acute topic of many research efforts (Puerta *et al.*, 2020). The variability of the Gulf Stream System and its connection to fisheries, and more generally to the regional marine ecosystem is now under the spotlight in many ecosystem research and review papers (Drinkwater, 2005; Drinkwater *et al.*, 2013a; Drinkwater *et al.*, 2013b; Harning *et al.*, 2021; Holt *et al.*, 2014; Kamykowski, 2014; Sherman *et al.*, 2013).

The aquatic environments are extremely sensitive to oceanographic conditions and to ongoing ocean and climate change (Barange and Harris, 2010; Blanchard *et al.*, 2012; Edwards *et al.*, 2022; Mann and Lazier, 2013). Especially important are coastal zones with exceptionally high biological productivity and high rates of biogeochemical cycling (Drinkwater *et al.*, 2009; Holt *et al.*, 2009). The migration of the frontal zones was a critical driver for marine ecosystem through ages, e.g., (Harning *et al.*, 2021).

The Northwest Atlantic in the vicinity of the U.S. and Canadian coastal zones has been the focus of intensive research linked to fisheries and ecological health of the coastal water (Barange and Harris, 2010; Gonçalves Neto *et al.*, 2021; Shackell *et al.*, 2014; Sherman *et al.*, 2013; Skjoldal and Sherman, 2002; Stenseth, 2004). A substantial effort has been made to find connections between ecosystem dynamics and variability with large-scale ocean circulation and major climate indices such as the North Atlantic Oscillation (NAO), Atlantic Multidecadal Oscillation (AMO),

etc. (Brander, 2010; Nye, 2010; Nye *et al.*, 2014; Overland *et al.*, 2010; Sarmiento *et al.*, 2004; Schmittner, 2005; Seidov *et al.*, 2017; Seip K.L *et al.*, 2019). Vulnerability of fisheries in the coastal zones of North America's eastern coast in response to ocean and climate change has been specifically addressed as a prime topic of fisheries-climate connections (Allison *et al.*, 2009; Brander, 2010; Jennings and Brander, 2010; Lehodey *et al.*, 2006; Puerta *et al.*, 2020; Sherman *et al.*, 2013).

As stated above, the NWA region is characterized by a very complex circulation pattern with fine-structured circulation and recirculation gyres, meandering jets, nonlinear baroclinic waves, meanders and rings strongly interacting with the Gulf Stream, Gulf Stream Extension, and the Labrador Current. Many research efforts point toward an intricate but clearly observed connection between biological indicators, such as chlorophyll and phytoplankton concentration and variability, and the eddy regime in the Gulf Stream System (Frajka-Williams *et al.*, 2009; Leterme and Pingree, 2008; Schollaert *et al.*, 2004). To provide a meaningful and useful observational oceanographic background for fisheries and ecosystem research, a spatial resolution that can resolve ocean jets, meanders, and the cumulative effects of mesoscale eddies with the grid sizes of just a few tens rather than hundreds of kilometers, is in strong demand.

Indeed, for an eddy with the size of 50 km, which is approximately half of the baroclinic Rossby wavelength, one-degree spatial resolution does not resolve this wavelength at all, while the quarter degree gives only five points per wavelength and thus provides just a borderline resolution of baroclinic eddies. The one-tenth-degree longitude-latitude grid, on the other hand, has 8 to 10 grid points in mid-latitudes and thus provides sufficient resolution for the spatial scales of the baroclinic Rossby deformation radius. Additionally, the seasonal cycle, which may have spatial shifts of currents of tens to hundreds of kilometers, is superimposed on interannual variability and is essential for all elements of marine ecosystems (e.g., (Leterme and Pingree, 2008; Skjoldal and Sherman, 2002). The decadal-scale changes in seasonal cycles are of paramount importance, especially for fish stocks in this dynamically complex and highly variable ecosystem. We can conclude, based on climate research and application demands, that selection of the NWA region for a more detailed analysis and mapping is timely and justified.

8. NORTHWEST ATLANTIC REGIONAL OCEAN CLIMATOLOGY

The NWARC v2 domain is the same as the domain of the NWARC v1 (Seidov *et al.*, 2016). It is bounded by 80.0°W and 40.0°W longitudes and 32.0°N and 65.0°N latitudes (see Figure 4). The NWARC v2 is comprised of analyzed temperature and salinity fields computed to map the mean state of the ocean in the NWA area and to assess long-term climatological tendencies in this important region. The set includes objectively analyzed temperature and salinity fields as well as some additional parameters that may be useful for applied climate studies, including simple statistical means, data distributions, standard deviations, standard errors of the mean, observed minus analyzed, and seasonal minus annual distributions for both temperature and salinity.

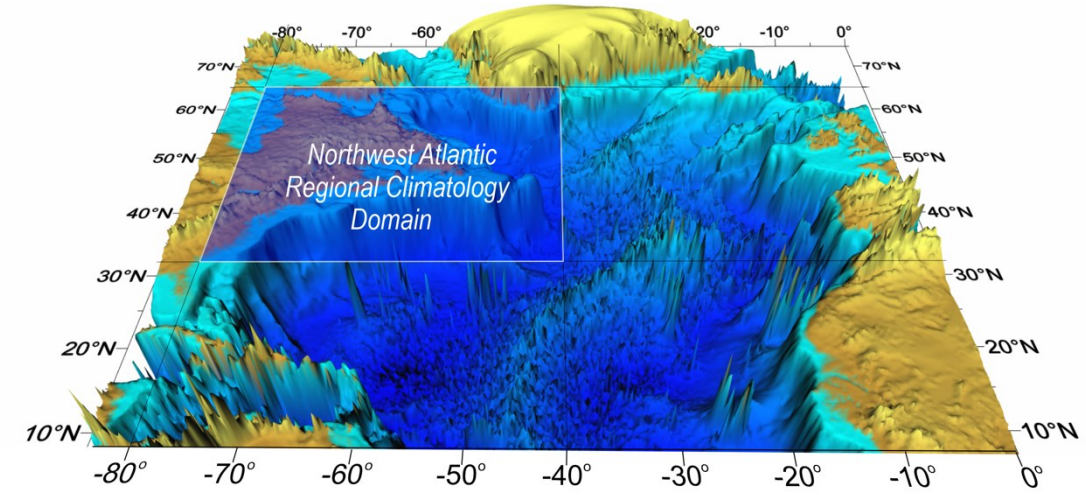

Figure 4. Bottom topography of the North Atlantic Ocean (ETOPO1 Global Relief Model from NOAA) with the outline of the NWA regional climatology area.

All data from the WOD18 between 1955 and 2017 in the NWARC v2 domain were used to calculate six decadal climatologies within the following time periods: 1955-1964, 1965-1974, 1975-1984, 1985-1994, 1995-2004, and 2005-2017 (Table 1). The averaged ~60-year climatology (*decav* – stands for *dec*adal *av*erage) was calculated by averaging the six individual decades listed above, e.g., (Boyer *et al.*, 2018a). For all three grid resolutions (one-, quarter-, and one-tenth-degree), mean depth values at the center of a grid square with the respective resolution were extracted from the ETOPO2 World Ocean bathymetry.

The NWARC v2 is designed similarly to WOA18, and therefore all characteristics of WOA18 also apply to NWARC. Hence, the following description of NWARC v2 mostly follows

WOA18 publications (Locarnini *et al.*, 2018; Zweng *et al.*, 2018b) and NWARC v1 publication (Seidov *et al.*, 2016). Specific features of NWARC v2 are addressed further in the text regarding the data coverage, objective analysis, and quality control in the NWA region.

All WOA editions prior to WOA18 were comprised of analyzed oceanographic parameters at 33 depth levels with just one spatial resolution of 1°x1°. As a major upgrade, WOA18 provided all fields on both one- and quarter-degree longitude-latitude grids with the extended vertical resolution of 102 depth levels. (Some statistical fields were computed on 5°x5° grid as well, the same as was done in previous editions).

The time span of decadal fields in WOA18 stretches over six decades from 1955 to 2017 (the last "decade" – the years 2005 to 2017 – covers thirteen years). Table 1 shows the time spans used in both WOA18 and NWARC v2 (see WOA18 Documentation for more details). The statistical and analyzed fields are annual, seasonal, and monthly providing a climatological year, four climatological seasons, and twelve climatological months for each decade.

Table 1. Time Spans in WOA18 and NWARC v2.

Time Span	Abbreviation	Comment
1955 – 1964	5564	First decade with sufficient data for climatological mean fields
1965 – 1974	6574	
1975 – 1984	7584	
1985 – 1994	8594	
1995 – 2004	95A4	The coverage includes Argo floats
2005 – 2017	A5B7	
1955 – 2017	*decav*	Average of six decadal means

In addition to the objectively analyzed fields, both WOA18 and NWARC v2 provide: (a) statistical mean fields, (b) the observation density (number of observations in each grid cell), and (c) other statistical parameters that help to assess ocean climate on all grids as shown in Table 2. More details can be found in the WOA18 Documentation.

Table 2. Available objectively analyzed and statistical fields in NWARC v2.

Field Name	1/10° field	1/4° field	1° field
Objectively analyzed climatology	√	√	√
Statistical mean	√	√	√
Number of observations	√	√	√
Seasonal or monthly climatology minus annual climatology	√	√	√
Standard deviation from statistical mean	√	√	√
Standard error of the statistical mean	√	√	√
Statistical mean minus objectively analyzed climatology	√	√	√

The statistical fields in NWARC v2 were calculated for only temperature and salinity, in contrast to WOA18 having calculations for six variables: temperature, salinity, dissolved oxygen, nitrate, phosphate, and silicate, albeit only on one-degree grid. Because different variables in the database have different levels of data coverage/data density (or sparsity), not all variables were analyzed at all depths for all averaging periods (annual, seasons and months) and time spans.

Table 2 shows fields of statistical and auxiliary variables included in NWARC. All fields are compiled at 102 standard depth levels for one-tenth-, quarter-, or one-degree spatial resolution grids. Here is a short description of those fields:

- Objectively analyzed climatologies: objectively interpolated mean fields for an oceanographic variable.
- The statistical mean: the average of all interpolated data values that pass quality control checks at each cell which contain at least one measurement for the given oceanographic variable.
- The number of observations of each variable in each grid cell at each standard depth level.
- The standard deviation from the statistical mean of each variable in each grid cell at each standard depth level.
- The standard error of the mean of each variable in each grid cell at each standard depth level.
- The seasonal or monthly climatology minus the annual climatology at each grid cell at each standard depth.
- The statistical mean minus the objectively analyzed climatological mean at each grid cell at each standard depth. This value is used as an estimate of interpolation and smoothing error.

Table 3. Depths associated with each standard level number in WOA13, WOA18, and NWARC v1 and v2 (bold numbers indicate standard levels used in earlier versions of WOA).

Depth (m)	Level	Depth (m)	Level	Depth (m)	Level	Depth (m)	Level
0	1	**250**	27	**1300**	53	3300	80
5	2	275	28	1350	54	3400	81
10	3	**300**	29	**1400**	55	**3500**	82
15	4	325	30	1450	56	3600	83
20	5	350	31	**1500**	57	3700	84
25	6	375	32	1550	58	3800	85
30	7	**400**	33	1600	59	3900	86
35	8	425	34	1650	60	**4000**	87
40	9	450	35	1700	61	4100	88
45	10	475	36	**1750**	62	4200	89
50	11	**500**	37	1800	63	4300	90
55	12	550	38	1850	64	4400	91
60	13	**600**	39	1900	65	**4500**	92
65	14	650	40	1950	66	4600	93
70	15	**700**	41	**2000**	67	4700	94
75	16	750	42	2100	68	4800	95
80	17	**800**	43	2200	69	4900	96
85	18	850	44	2400	71	**5000**	97
90	19	**900**	45	**2500**	72	5100	98
95	20	950	46	2600	73	5200	99
100	21	**1000**	47	2700	74	5300	100
125	22	1050	48	2800	75	5400	101
150	23	**1100**	49	2900	76	**5500**	102
175	24	1150	50	**3000**	77		
200	25	**1200**	51	3100	78		
225	26	1250	52	3200	79		

All depth levels are shown in Table 3, with the standard depth levels used in previous version of WOA shown in bold.

As shown in Table 4, the monthly climatology is defined for the upper 57 levels only because of sparseness of monthly data below 1500 m.

Table 4. Depth ranges and the number of standard depth levels for the statistics of temperature and salinity.

Oceanographic Variable	Depths for Annual Climatology	Depths for Seasonal Climatology	Depths for Monthly Climatology
Temperature and Salinity	0-5500 meters (102 levels)	0-5500 meters (102 levels)	0-1500 meters (57 levels)

Seasonal and annual means were computed as averages of monthly fields above 1500 m and as averages of all data for seasonal fields below. The annual fields were computed by averaging the seasonal fields. There is almost no seasonal cycle signal below 1500, except for the region of deep convection, with the convection intensity depending on seasons.

Table 5. Number of temperature profiles in NWA region for each decade from 1955 to 2017.

Temperature	1955-1964	1965-1974	1975-1984	1985-1994	1995-2004	2005-2017	1955-2017
January	8,983	11,448	7,811	6,402	5,840	12,445	52,929
February	10,863	10,829	9,618	7,935	7,627	13,129	60,001
March	12,654	16,822	13,866	10,018	9,016	19,167	81,543
April	17,233	18,749	15,956	11,574	28,920	20,604	113,036
May	21,459	24,126	18,461	14,102	35,510	23,529	137,187
June	24,191	23,163	19,245	14,225	17,539	18,372	116,735
July	23,400	24,875	19,824	12,534	18,061	31,943	130,637
August	22,625	25,662	20,115	14,618	17,531	38,749	139,300
September	18,134	22,860	15,640	11,643	14,623	52,662	135,562
October	15,534	20,409	18,218	11,437	14,863	40,393	120,854
November	16,736	18,314	15,422	13,110	15,371	19,821	98,774
December	10,635	10,977	7,156	7,114	10,415	13,269	59,566
Total NWARC v2	*202,446*	*228,234*	*181,326*	*134,711*	*195,315*	*304,083*	*1,246,116*
Total NWARC v1	*(202, 446)*	*(228,260)*	*(181,396)*	*(124,887)*	*(149,610)*	*(81,705)*	*(968,304)*

Tables 5 and 6 show the number of temperature and salinity profiles held in WOD18 (after automatic and manual quality control performed) within the NWA borders by months for each

decade and for entire 1955-2017 period. Thus, all temperature profiles in all casts made in each January of each year of the 1955-1964 decade are shown as January profile numbers in Tables 5 and 6. The rightmost column shows total profiles count from 1955 to 2017.

Table 6. Number of salinity profiles in NWA region for each decade from 1955 to 2017.

Salinity	**1955-1964**	**1965-1974**	**1975-1984**	**1985-1994**	**1995-2004**	**2005-2017**	**1955-2017**
January	858	2,396	3,207	2,757	3,303	7,064	*19,585*
February	1,254	2,473	3,309	3,155	5,084	6,934	*22,209*
March	1,493	3,544	5,040	4,257	5,703	13,317	*33,354*
April	2,976	5,832	6,161	6,585	25,239	15,928	*62,721*
May	2,744	6,395	7,348	7,657	31,538	19,260	*74,942*
June	3,355	6,761	8,085	7,269	8,591	15,393	*49,454*
July	4,082	7,690	10,430	7,808	10,248	29,017	*69,275*
August	3,910	7,811	10,133	8,947	10,024	35,893	*76,718*
September	2,270	5,573	6,417	6,744	8,861	49,992	*79,857*
October	1,609	4,343	6,708	6,810	8,224	37,088	*64,782*
November	1,663	4,307	5,566	7,192	8,474	15,546	*42,748*
December	,891	1,992	2,574	3,664	4,518	9,788	*23,427*
Total NWARC v2	*27,105*	*59,117*	*74,978*	*72,845*	*129,807*	*255,220*	*619,072*
Total NWARC v1	*(27,105)*	*(59,134)*	*(75,085)*	*(63,010)*	*(112,402)*	*(67,066)*	*(403,802)*

Data density is generally quite high; in fact, the data coverage is much denser in the NWA domain than in most of the World Ocean. Nonetheless, the availability of temperature and salinity profiles varies in space and time within the NWA domain quite substantially, and there is also a significant variation of data availability between the decades and between the seasons in each decade.

Figures 5a,b illustrates the monthly coverage in the six decades. Tables 5 and 6 and Figure 5 reveal an interesting tendency that could not have been anticipated *a priori*, namely, a decreasing number of in situ observations in the NWA over the period of record, except for the last decade of 2005-2017, when the number of observations exploded.

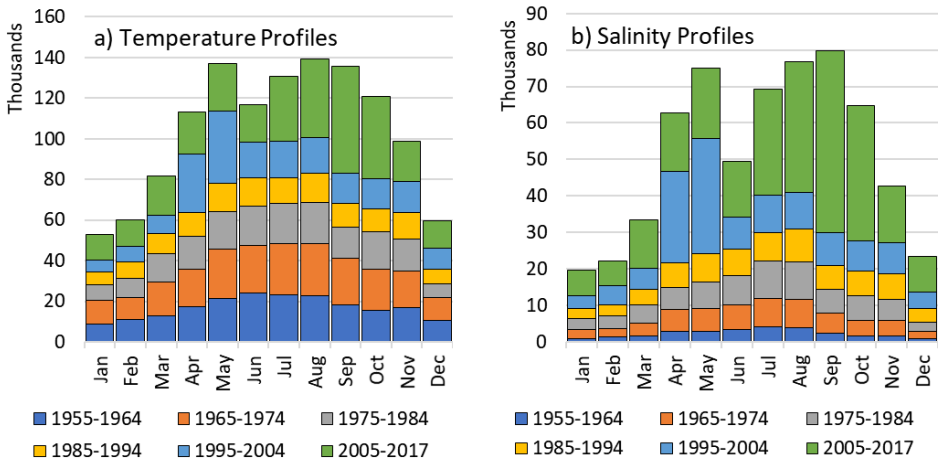

Figure 5. Number of (a) temperature and (b) salinity profiles in NWA region for each month of each decade from 1955 to 2017.

Even considering that the last "decade" is three years longer than others, the increase of the temperature observation numbers is notable—over 100,000 more than in the previous decade of 1995-2004. Adjusted for the extended duration of the last "decade", the number of profiles is still somewhat smaller than in the 1965-1974 period, when the Gulf Stream region was most intensively observed (Yashayaev *et al.*, 2015). Comparison of temperature and salinity by instruments gives a hint to why the number of observations has decreased in recent years, and why the last decade shows such impressive increase of profiles. Tables 7 and 8 (Figures 6a,b) show the number of temperature and salinity profiles, respectively, for each of the six decades obtained using different instruments.

Table 7. Number of temperature profiles in NWA region for each decade from 1955 to 2017 by instrument (see text).

Instrument	1955-1964	1965-1974	1975-1984	1985-1994	1995-2004	2005-2017	1955-2017
OSD	29,475	59,648	60,187	22,974	3,472	3,343	*179,099*
MBT	172,971	113,457	22,343	15,363	42		*324,176*
XBT		51,693	76,021	44,936	28,492	21,492	*222,634*
CTD		3,436	22,767	41,457	59,600	64,837	*192,098*
APB					28,031	28,235	*56,266*
PFL				20	17,626	45,813	*63,459*
UOR			8	9,961	55,942	9,787	*75,698*
GLD					2.110	130,576	*132,686*
Total	*202,446*	*228,234*	*181,326*	*134,711*	*195,315*	*304,083*	*1,246,116*

Table 8. Number of salinity profiles in NWA region for each decade from 1955 to 2017 by instrument (see text).

Instrument	1955-1964	1965-1974	1975-1984	1985-1994	1995-2004	2005-2017	1955-2017
OSD	27,105	55,901	53,860	21,953	3,205	3,218	*165,242*
CTD		3,216	21110	40,930	59,007	64,718	*188,981*
APB						1,777	*1,777*
PFL				1	9,654	45,787	*55,442*
UOR			8	9,961	55,833	9,787	*75,589*
GLD					2,108	129,933	*132,041*
Total	*27,105*	*59,117*	*74,978*	*72,845*	*129,807*	*255,220*	*619,072*

In Tables 7 and 8 and Figure 6, the abbreviations stand for: OSD–Ocean Station Data (bottles); MBT–Mechanical Bathythermograph; XBT–Expendable Bathythermograph; CTD–Conductivity-Temperature-Depth; PFL–Profiling Float; UOR–Undulating Oceanographic Recorder; GLD–Glider (see text), APB- Autonomous Pinniped Bathythermographs. Note that we do not show the data from MRB (Moored Buoys) because they provide large amounts of data, but in fixed locations, whereas all other instruments are responsible for areal coverage (i.e., MRB data are included in the NWARC, but are not accounted for in the Tables and Figures).

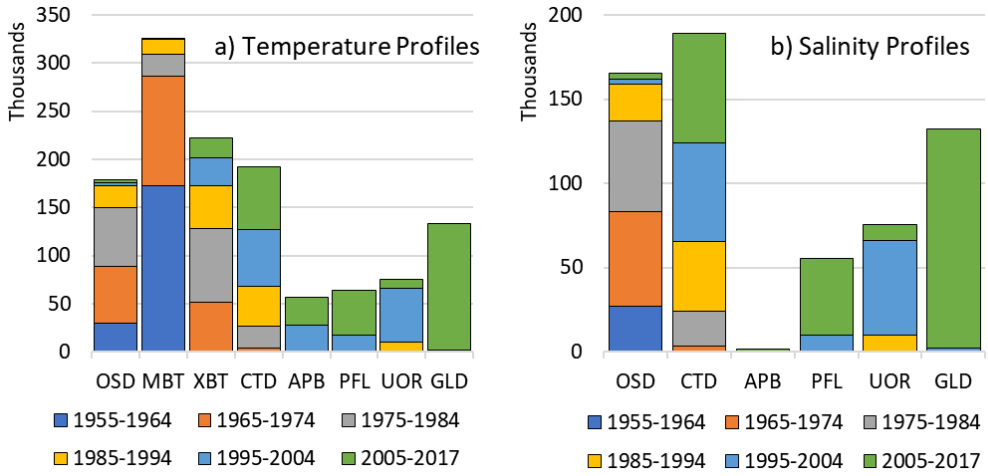

Figure 6. Number of (a) temperature and (b) salinity profiles in NWA region for each decade per instrument.

In Tables 5 and 6, the total number of profiles available in NWARC v1 is shown in brackets below the total number of the profiles available in the updated NWARC v2. As Tables 5 and 6

reveals, there is a substantial increase in total profiles in the NWARC v2 compared to NWARC v1. While the very substantial increase of the data amount happened in the last "decade" of 2005-2017, which is 5 years longer in NWARC v2 than the "decade" of 2005-2012 in NWARC v1, this increase is still very substantial in previous decades as well. Overall, total number of the profiles used in all decades is much higher in NWARC v2 compared to NWARC v1 (1,246,116 vs. 968,304 for temperature; 619,072 vs. 403,802 for salinity). That is, in total, there are 277,812 new temperature and 215,270 new salinity profiles added to the new version of the NWA regional climatology. (Note: the small reduction of the number of the profiles in the 1965-1974 period is due to WOD duplicate records removal.

As the older instruments, like MBT, left the scene and the new ones, like PFL (which is mainly Argo), come in use, the number of profiles per decade in the region changed accordingly. This is another caveat of replacing onboard measurements (e.g., from ships or stationary buoys) with data from passive drifters of any type. Both are important and should be used concurrently rather that interchangeably. Argo floats, or any drifters for that matter, are not designed to target specific sites or provide specific regional coverage as they tend to disperse and follow circulation patterns rather than to remain in a selected region, as would be the case in the in situ observations from ships or stationary buoys. Contrasting to ship-based observations usually targeting specific regions, the drifters tend to cover some regions more homogeneously, with lesser observation density in specific areas, which may or may be not the desired outcome depending on research goals. Tables 7 and 8 and Figure 6 reveal the surge in PFL profiling during the last 13 years. In 2005-2017 there were 45,813 PFL observations in the NWA region—compared to 17,626 in the previous decade. The future of in situ observational oceanography clearly leans toward the overwhelming dominance of Argo and other autonomous probes like gliders.

Figure 7 shows data coverage for two decades in the NWA region on the one-degree grid. Figure 7a (left) shows the density of temperature observations at 10 m depth for the decade of 1965-1974, while Figure 7b (right) displays the density of observations for 1995-2004.

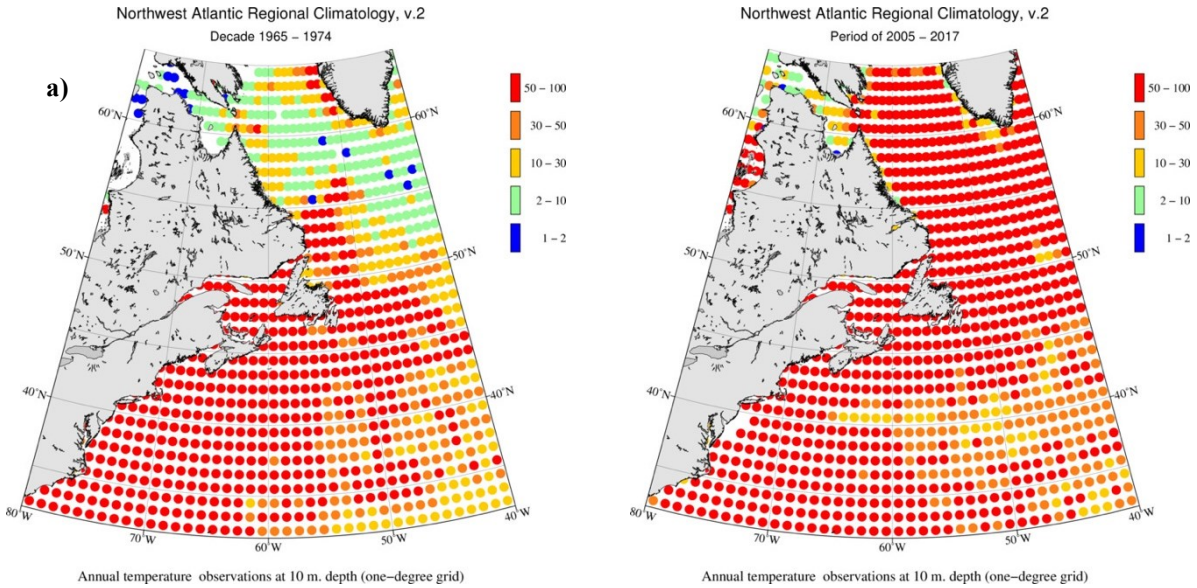

Figure 7. Density of annual temperature observations (number of observations per grid box) at 10 m depth for periods of (a) 1965 - 1974 and (b) 2005 – 2017 within one-degree grid boxes.

Figures 8a and 8b shows the temperature data distribution but on the one-tenth-degree grid. (Entire collection of maps showing data coverage of both temperature and salinity for all climatological months, seasons, and years at all depths can be found at the NWARC v2 website).

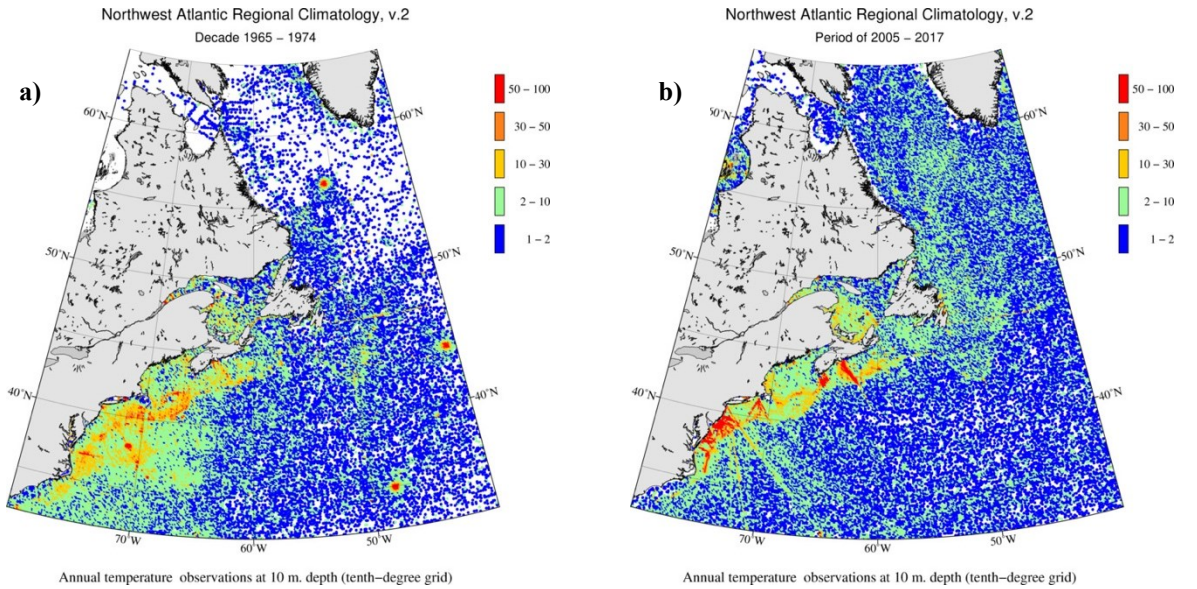

Figure 8. Density of annual temperature observations (number of observations per grid box) at 10 m depth for periods of (a) 1965 – 1974 and (b) 2005 – 2017 within one-tenth-degree grid boxes.

There are much fewer spatial gaps between observations or empty cells in the more recent decade of 2005-2017 than in the earlier decade of 1965-1974, particularly at higher latitudes. However, the U.S. coastal area and the Gulf Stream area were noticeably better covered by observations in 1965-1974 than in 1995-2004, where many massive oceanographic programs were conducted at that time (Yashayaev *et al.*, 2015). That is, modern technology helps to cover wider areas, often under sampled by traditional instruments, especially away from the coastline in rogue weather area, but at the expense of fewer focused observations which were characteristic of the earlier decades where intensive studies of the Gulf Stream in the 60's and 70's and mesoscale ocean eddies in the 70's and 80's occurred. On the other hand, the finer resolution is better facilitated by newer technology that helps to close the gaps and allows compiling high-resolution regional climatologies, as in the NWA case (see Tables 7 and 8). For example, the Labrador Sea is far better covered in 1995-2004 when compared to 1965-1974 (Figures 7a and 7b), with improved coverage due to introduction of Argo floats and gliders. At the same time the Gulf Stream between the Florida Strait and Cape Hatteras was better covered in 1965-1974, when many special programs studying the Gulf Stream were conducted (compare Figures 5a and 5b). Obviously, there are more PFL and GLD profiles in 2005-2017, also because this "decade" has 13 years covered (see Tables 7 and 8 and Figure 6), yet mostly because the PFL and GLD are becoming the most advanced and common modern observing instruments.

Even in the very well covered NWA region, there are more profiles in summer than in winter (Tables 5 and 6 and Figure 5 above), and within months there are noticeable differences between colder and warmer months. If the seasonal or annual fields were calculated using all annually and seasonally available profiles, they may become biased toward warmer months within seasons and to summer months in annual average. Such bias in data collecting pattern is because marine expeditions more often planned for the seasons with better weather conditions. To alleviate such a possibility, the new approach to aggregating data using climatological months to compute climatological seasons and years was used for the first time in both WOA13 and NWARC v1 and then continued in WOA18 and all regional climatologies after NWARC v1 (see Figure 1). The seasonal fields are computed as the average of three months comprising each season, and the annual fields are computed as the average of four seasons. Although monthly fields are computed at all levels and principally could have been used to calculate seasonal fields at all levels, in the NWARC v2 the monthly fields are used to compute seasons and are shown only in the upper

1500m, while seasonal fields are computed using all data within a season and shown below 1500m. The caveats of using monthly and seasonal fields in the deep ocean will be discussed further.

Notably, NWARC v2 has one-tenth-degree spatial resolution for annual, seasonal, and monthly temperature and salinity fields for all six decades. The compilation of fields at such high resolution in both temperature and salinity provides a tool for assessing high-resolution ocean climate records based solely on historical in situ hydrographic observations over sixty years, which is twice the WMO-recommended climate definition length. Moreover, the quality control on a higher-resolution grid reveals more outliers than on coarser resolution grids, as more observed profiles are found within fronts, stationary meanders, etc. Compared to lower resolution, the structure of the gridded fields with one-tenth-degree resolution is far better captured, especially in areas with sharp gradients of the essential oceanographic parameters (temperature, salinity, etc.). Such gradients and other persistent mesoscale features are better preserved in the generated climatological fields, which makes high-resolution climatologies more valuable for ocean modeling and other applications. (Importantly, were they not persistent, mesoscale features would have been filtered out by decadal averaging, even at high spatial resolution; see the discussion in Chapter 11).

To summarize, the NWARC v2 is an important update of the NWARC v1, which itself was a major new step toward assessing the high-resolution regional ocean climate. When compared to previous regional ocean climate reconstructions that provided aggregated regional climatologies averaged over the entire time span of available observations, NWARC v2 offers six annual, seasonal, and monthly decadal climatologies and presents both temperature and salinity on one-tenth-degree grid. Breaking the one-tenth degree barrier enables the NWARC v2 to shed some important new light on decadal-scale ocean climate variability in the NWA region based on in situ oceanographic observations rather than on ocean modeling with the same (sometimes just slightly finer) resolution. Additionally, the finer resolution allows tracking changes in mesoscale features over the last six decades.

In other words, the high-resolution NWARC v2 provides the means to study long-term thermohaline decadal variability with a grid resolution comparable with eddy-resolving numerical models of the Gulf Stream System.

9. NWARC v2 DATA PROCESSING AND OBJECTIVE ANALYSIS

This section provides a summary of how profile data from WOD are processed to create a gridded climatology following the in-detail descriptions in the Temperature and Salinity volumes of the WOA18 (Locarnini *et al.*, 2018; Zweng *et al.*, 2018b). For further information on the data sources used in WOA18 and detailed descriptions of the methods and techniques, which are fully applicable to NWARC, can be found in (Boyer *et al.*, 2018a).

To understand the procedures for taking individual oceanographic observations and constructing climatological fields, it is necessary to define the terms "standard level data" and "observed level data." We refer to the actual measured value of an in situ oceanographic variable as an "observation", and to the depth at which such a measurement was made as the "observed level depth." We refer to such data as "observed level data." All standard depth levels used in WOA18 and in NWARC v2 are listed in Table 3 (see above). The procedure of interpolating data from actual depths of observations onto the standard depths is described in the WOA18 documentation (Boyer *et al.*, 2018b; Locarnini *et al.*, 2018; Zweng *et al.*, 2018b).

Quality control of the temperature and salinity data is a major task, the difficulty of which is directly related to availability of data and metadata upon which to base statistical checks. The quality of oceanographic datasets and their usability for a given application critically depend on the data coverage. Data coverage as used here is not just the volume of data in the region, but refers particularly to the spatial distribution of data, which is the key indicator of the quality of the data set used to obtain climatological means. The data coverage varies hugely in different regions of the World Ocean. Thus, the success of compiling a meaningful and useful regional climatology critically depends on how much data are available and how they are distributed in a selected domain. Fortunately, as was mentioned above, the NWA region is one of the best data-covered regions of the World Ocean thus giving an optimism for compiling a meaningful high-resolution regional decadal climatology. It can therefore be anticipated that NWARC v2 will provide solid oceanographic foundation for ocean climate studies and numerous practical applications with embedded dependencies on long-term ocean climate change.

The data used in ocean climatology calculations needs to be pre-processed to ensure the quality of the gridded and analyzed fields. First, duplicate profiles and obvious outliers must be removed prior to visual inspection and final manual quality control preceding climatology

compilation. Because both in situ temperature and salinity data are received from many sources, it is possible that, in some instances, the same data set is received at the NCEI archived more than once but with slightly different time and/or position and/or data values due to different generalization and rounding applied by data originators, and hence are not easily identified as duplicate stations. To eliminate the repetitive data values, WOD is constantly being checked for the presence of exact and "near" exact duplicates using a several sets of different criteria combination. The initial set of checks involve identifying stations with exact position/date/time and data values; the next checks involve offsets in position/date/time. Profiles identified as duplicates in the checks with a large offset were individually verified to ensure they were indeed duplicate profiles.

Range checking (i.e., checking whether a measured value is within a preset minimum and maximum limits as a function of depth and ocean region) was performed on all temperature and salinity values as a first quality control check to flag and withhold from further use the relatively few values that were grossly outside expected oceanic ranges. The procedure is detailed in Johnson *et al.* (2013).

As summarized in WOA18 publications, e.g., (Locarnini *et al.*, 2018), first the five-degree square statistics were computed, and the data flagging procedure was used to provide a preliminary data set. Each five-degree square box was designated as coastal, near-coastal, or open ocean, depending on the number of one-degree latitude–longitude grid boxes in the five-degree box which were land areas. The data exceeding three, four and five standard deviations in the open-ocean, near-coastal and coastal areas, respectively, were flagged to be excluded from computing and re-computing the climatology.

After the first cleaning of data is completed and outliers marked, the one-degree square statistics are computed, and the data flagging procedure described above was used to form a preliminary data set. Next, new one-degree-square statistics were computed from this preliminary data set and used with the same statistical check to produce a new, cleaner data set. At the first step of the two-step statistical check any grossly erroneous or non-representative data are found and flagged. At the second step, the values with smaller differences that are still non-representative are found and marked.

Each cast containing both temperature and salinity was checked for static stability, *E*, as used by (Lynn and Reid, 1968) and is given by:

$$E = \lim_{\delta z \to 0} \frac{1}{\rho_0} \frac{\delta \rho}{\delta z} \tag{1}$$

where: ρ_o= 1.02 kg·m^{-3}.

As noted by Lynn and Reid (1968), static stability "is the individual density gradient defined by vertical displacement of a water parcel (as opposed to the geometric density gradient). For discrete samples the density difference (δρ) between two samples is taken after one is adiabatically displaced to the depth of the other". For the results at any standard level (k), the computation was performed by displacing parcels at the next deeper standard level (k+l) to level k.

The final and most time-consuming step in pre-processing the data to build a decadal or any other climatology is subjective manual flagging of data, where the data are contour-plotted and so-called “bullseyes” are visually detected and marked to remove the data from part of the profiles or sometime the entire profiles from subsequent recalculation of the climatology, or “climatology re-run.” The quality control for the NWARC v2 was done on three grids: a one-, a quarter-, and a one-tenth-degree grid. For the one-degree analysis, the temperature and salinity data were averaged by one-degree cells for input to the objective analysis program. After initial objective analyses were computed, the input set of one-degree means still contained questionable data contributing to unrealistic features, yielding intense “bullseyes” or unlikely spatial gradients. If bullseyes or unrealistic gradients were found the data were flagged. The procedure was repeated for the quarter- and one-tenth-degree grids.

After subjective manual quality control procedures were completed on all grids for all decades, the new first guess field was calculated on a one-degree grid and then all climatologies were recomputed and the objective analysis was performed on all grids and all accompanied statistics were recalculated. The first-guess field for each of these climatologies is the temperature and salinity fields compiled using all available data.

Summarizing, the zonal mean fields are used as the first guess for compiling one-degree fields. Then one-degree fields are used as the first-guess field for compiling one-quarter- and after

that the quarter degree fields are used as the first guess for compiling the one-tenth degree fields. Usually, several iterations of manual quality control and subsequent climatology re-run procedure was executed to ensure the best possible quality within reasonable time and effort.

Data processing procedures comprise the entire sequence of steps resulting in compiling a climatology or a set of climatologies. The NWARC v2 contain six decadal climatologies, and *decav* (the average of six decadal) climatology. Compilation of the climatologies consists of several technical sub-procedures described in depth in a number of WOA publications and in some research papers based on various versions of WOA, e.g., (Boyer *et al.*, 2005; Levitus *et al.*, 2012; Locarnini *et al.*, 2018; Seidov *et al.*, 2015; Zweng *et al.*, 2018a).

The NWARC, like all previous versions of WOA and all regional climatologies, was built using a procedure widely known in geophysics as objective analysis of irregularly distributed data (Thomson and Emery, 2014). The objective analysis scheme adopted in all editions of WOA since WOA98 was introduced in (Barnes, 1964) and then updated in (Barnes, 1973) and (Barnes, 1994). Here, an objective analysis scheme as implemented at NCEI is described. A three-pass correction is used that begins with a ‘‘first-guess’’ field, which are full 360-degree (i.e. around the globe) zonally averaged temperature or salinity fields for each one-degree latitudinal belt. The second step is finding all data that are available within an influence radius around the center of the grid cell being analyzed. The correction to the first-guess values at all grid points is then computed as a distance-weighted mean of all grid point difference values that lie within the influence radius. This correction procedure is repeated twice more, each time with a decreasing search radius, for a total of three passes.

The idea behind the use of the influence radius in the objective analysis scheme used, can be briefly outline following (Levitus, 1982; Levitus *et al.*, 2012) and (Locarnini *et al.*, 2018). For computing the objectively analysed values of an oceanographic parameter, e.g., temperature, salinity, etc., on the one-degree grid, at each standard depth level all data within each one-degree grid cell are averaged a first-guess values are subtracted to produce a mean anomaly value. A definition of an influence region is introduced based on an influence radius, $\boldsymbol{R}$, around each one-degree cell to compute a “correction” using all one-degree square values in the influence region based on a Gaussian-shaped, distance-related weight function. At each one-degree cell, the correction is added to the first-guess field to produce an “analyzed” value. The goal of the entire

procedure is to fill all gaps in data coverage and produce relatively smooth yet realistic fields of ocean variables on a regular grid.

More details about the objective analysis scheme used to generate the climatological fields can be found in the WOA documentation (Antonov *et al.*, 2010; Locarnini *et al.*, 2010; Locarnini *et al.*, 2018; Zweng *et al.*, 2018b) and in the related publications (e.g., (Boyer *et al.*, 2005; Levitus *et al.*, 2012). In addition to the WOA documentation cited above, the mathematical background of the technique is revisited in the Appendix of the above cited publication by (Levitus *et al.*, 2012). The Appendix in Levitus *et al.* (2012) also provides a description of how the statistical errors of an objectively analyzed gridded field can be estimated using a general formula for error propagation (Taylor, 1997).

The influence radius is different for different grid resolutions and varies in the three-pass objective interpolation procedure for one, one-fourth and one-tenth degree grids respectively (see Table 9; more detailed explanation in the next section).

Table 9. Radii of influence used in objective analysis for one-degree, quarter-degree and one-tenth-degree NWA climatologies.

Pass Number	1° Radius of Influence	1/4° Radius of Influence	1/10° Radius of Influence
1	892 km	321 km	253 km
2	669 km	267 km	198 km
3	446 km	214 km	154 km

Thus, as seen in Table 9, the influence radius in one-tenth-degree resolution is 30% shorter than the quarter-degree one, which allows influence from a more geographically compact region with finer resolution of the objectively analyzed field, if the data availability is high (as in most regions of the NWA). In a way, if compared to numerical models, shortening the radius of influence is similar to decreasing the lateral turbulent mixing causing sharper current and more pronounced mesoscale hydrography structures. Importantly, the influence radius, and the number of five-point smoothing passes can be varied in each of the three sequential iterations in the three-pass variation of the implemented objective analysis procedure. The strategy is to begin the

analysis with a large influence radius and decrease in each of the subsequent iterations. This technique allows analysis of progressively smaller scale phenomena in subsequent iterations.

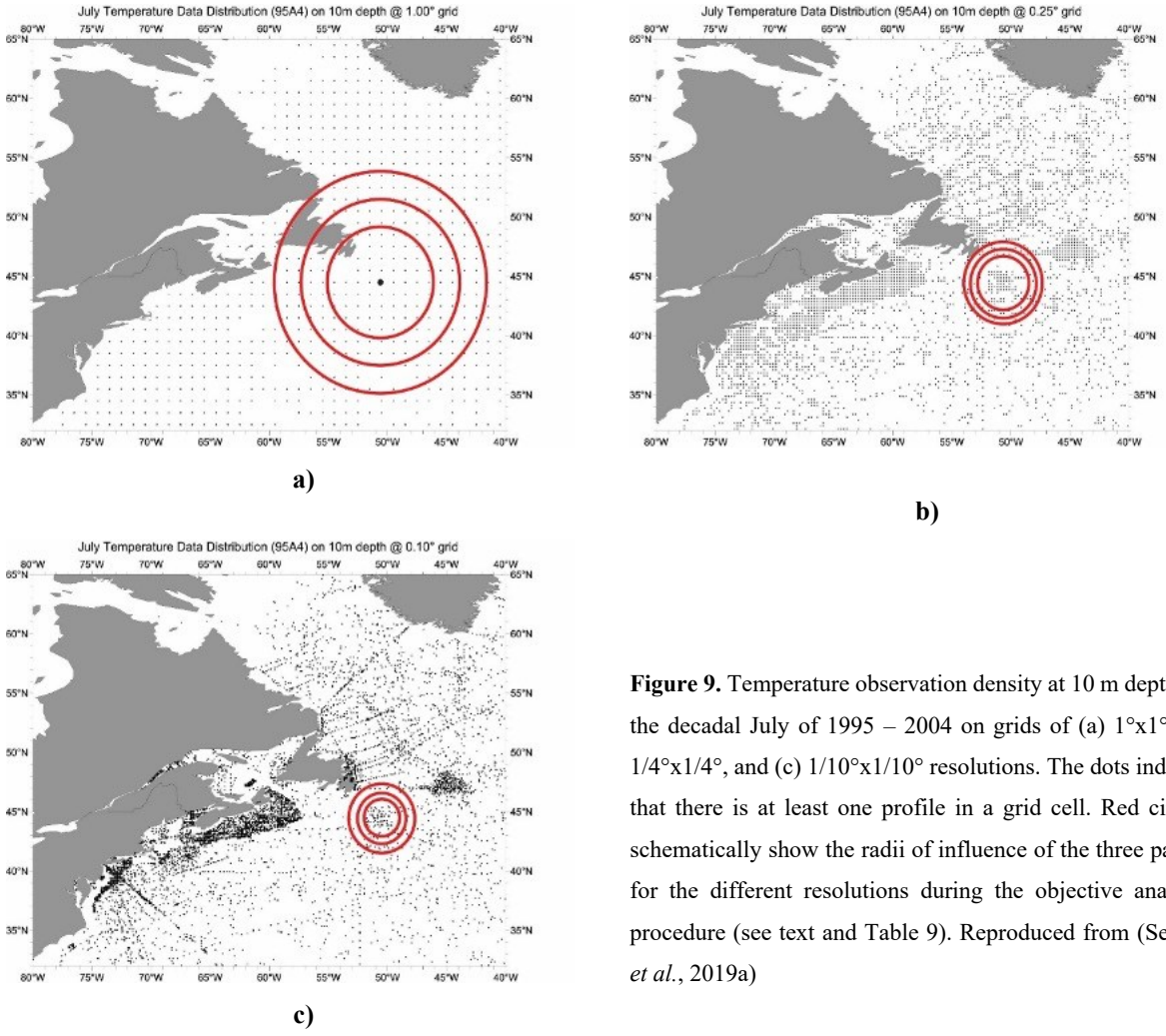

Figure 9. Temperature observation density at 10 m depth for the decadal July of 1995 – 2004 on grids of (a) 1°x1°, (b) 1/4°x1/4°, and (c) 1/10°x1/10° resolutions. The dots indicate that there is at least one profile in a grid cell. Red circles schematically show the radii of influence of the three passes for the different resolutions during the objective analysis procedure (see text and Table 9). Reproduced from (Seidov *et al.*, 2019a)

One of the most important parameters of this technique is the radius of influence (discussed in more detail in the next chapter), which essentially defines the area surrounding a grid cell from which the data are taken for interpolation to the cell center. Within the radius of influence, data points closer to the cell center are assigned higher weights. The robustness of the interpolation improves with increasing amounts of data inside the radius of influence. The radii of influence in the three-pass objective analysis on the one-tenth-degree grid is 50% to 40% shorter than on one-degree and by 34% to 13% shorter than on quarter-degree grid, e.g., (Boyer *et al.*, 2005; Locarnini *et al.*, 2018; Seidov *et al.*, 2015). Importantly, the radii of influence on a one-tenth-degree grid are on the scale of the Rossby baroclinic deformation radius of ~ 50 km in mid latitudes and even

shorter in subpolar and polar regions. For quarter-degree resolution, the radius of influence is comparable with Rossby baroclinic deformation radius characterizing mesoscale eddies, whereas this radius is greater than the cell sizes for one-tenth-degree resolution in mid-latitudes. Having cell sizes shorter than Rossby radius facilitates better statistics and more realistic patterns in the areas with high mesoscale activity (e.g., high variance is better captured around the fronts and shelf breaks).

Figure 9 illustrates how much finer details were achieved by decreasing the radius of influence and thus allowing mesoscale features to be captured by the analysis.

After computing the first-guess fields, the temperature and salinity data were re-analyzed using the newly produced analyses as first-guess fields described as follows. As was mentioned above, a new annual mean was computed as the mean of all 12 monthly analyses for the upper 1500 m, and the mean of the four seasons below 1500 m depth. This new annual mean was used as the first-guess field for new seasonal analyses. These new seasonal analyses in turn were used to produce new monthly analyses yielding slightly smoother means. The monthly mean objectively analyzed temperature fields were used as the first-guess fields for each of the "decadal" monthly climatologies. Likewise, seasonal, and annual climatologies were used as first-guess fields for the seasonal and annual decadal climatologies.

In some cases, data-sparse regions are so large that a seasonal or monthly analysis in these regions is meaningless. On the contrary, the geographic distribution of observations for the "all-data" annual periods (for example, see appendices in (Locarnini *et al.*, 2018)), has very little gaps and for the task of objective analysis it covers the World Ocean almost entirely. For the NWA region, the data distribution for "all-data" is especially dense, at least in the upper layers of the ocean. By using an "all-data" annual mean first-guess field, regions where data exist for only one season or month will show no contribution to the annual cycle. By contrast, if we used a zonal average for each season or month, then, in those latitudes where gaps exist, the first-guess field would be heavily biased by the few data points that exist. If these were anomalous data in some way, an entire basin-wide belt might be affected.

One advantage of producing "global" fields for a particular compositing period (even though some regions are data-sparse) is that such analyses can be modified by investigators for use in modeling studies. Moreover, the descendant regional climatologies, in this case the

NWARC, use more "time-granular" fields that are another strong advantage of the granular global approach.

Special care is needed near the domain boundaries, i.e., ocean coastal zones and near the bottom. Thus, corresponding masks are to be used while gridding the data. The analyses employed in the NWARC v2 use ETOPO2 land-sea topography to define ocean depths at each grid-point (ETOPO2, 2006). From the ETOPO2 land mask, a quarter-degree land mask was created based on ocean bottom depth and land criteria. The details of the masks in the WOA18 can be found in (Locarnini *et al.*, 2018).

The workflow of computing NWARC v2 seasonal and annual fields that includes density stabilization briefly outlined in this chapter is shown in Figure 10. Detailed discussion of the entire processing cycle can be found in (Locarnini *et al.*, 2018; Zweng *et al.*, 2018b).

As was mentioned above, the density field computed using temperature and salinity must be stabilized according to the Equation 1. Temperature and salinity climatologies are calculated separately, as there are some profiles with salinity measurements that are not always paired with temperature measurements and vice versa. As a result, when density is calculated from standard level climatologies of temperature and salinity, instabilities may result in the vertical density field (stability defined in previous section). While instabilities do occur in the ocean on an instantaneous time frame, these instabilities are usually short-lived and not characteristic of the mean density field. The stabilization of density is done globally in WOA and thus is not described here in detail. The Appendices A (Section 8.1) and B (Section 8.2) in (Locarnini *et al.*, 2018) describe a technique that was employed to minimally alter climatological temperature and salinity profiles in order to achieve a stable water column everywhere in the world ocean. The technique is based on the method of (Jackett and Mcdougall, 1995). The final temperature and salinity climatologies reflect the alterations due to this process.

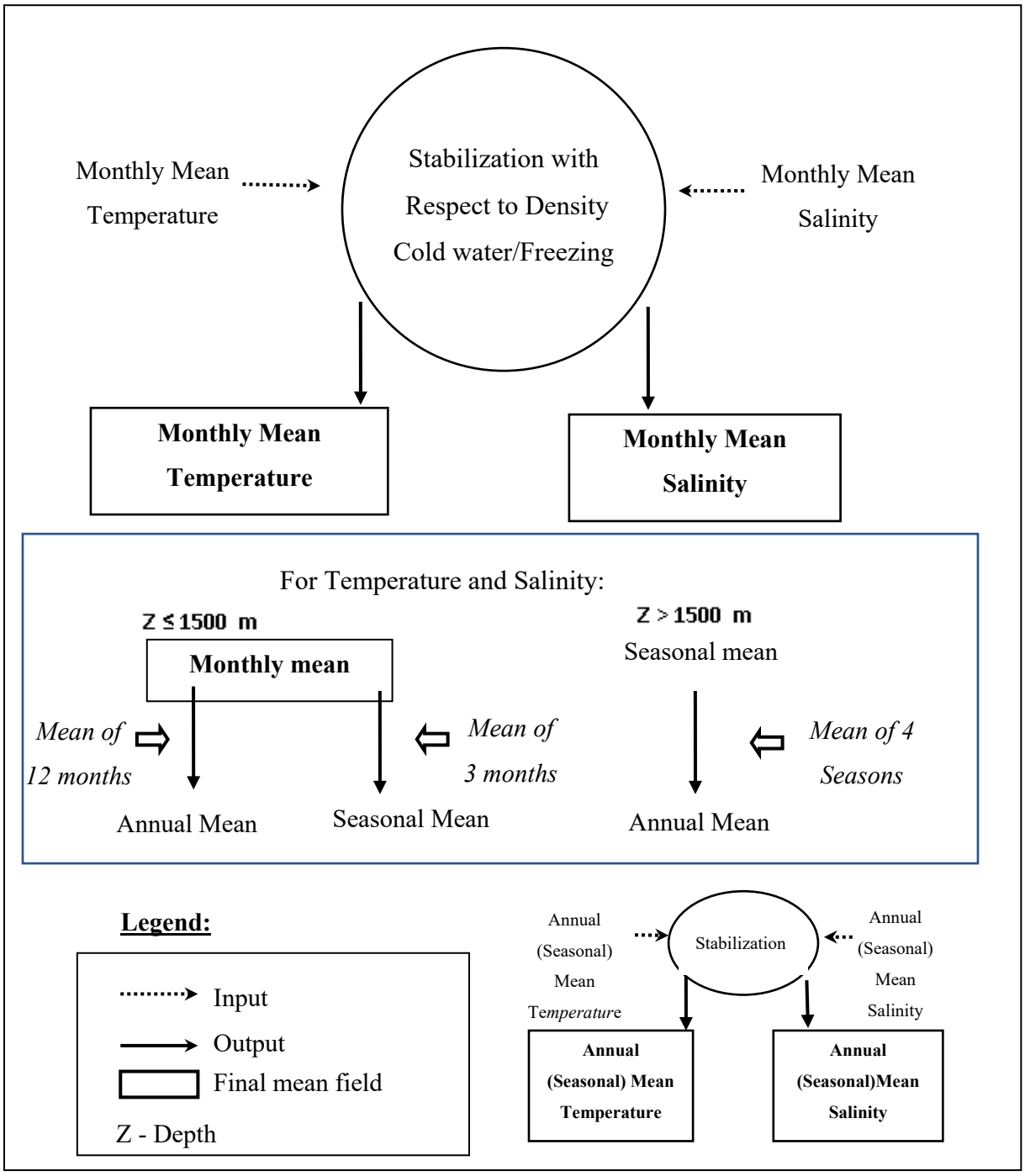

Figure 10. Scheme used in computing annual, seasonal, and monthly objectively analyzed means for temperature and salinity (from Locarnini et al., 2018).

10. ONLINE NWARC v2 MAPS AND DATA

The maps are arranged by composite time periods: annual, seasonal, and monthly. Table 2 (Section 8) lists all objective and statistical fields included in the NWA regional climatology set. All climatological maps of the objectively analyzed fields, and associated statistical fields at all standard depth levels are available online NWARC v2.

The sample standard deviation in a grid-box was computed using:

$$s = \sqrt{\frac{\sum_{n=1}^{N}(x_n - \bar{x})^2}{N-1}} \tag{2}$$

where x_n = the n-th data value in the grid-box, $\bar{x}$= mean of all data values in the grid-box, and N = total number of data values in the grid-box. The standard error of the mean was computed by dividing the standard deviation by the square root of the number of observations in each grid-box.

All objectively analyzed fields and all statistical data fields can be obtained online in ASCII comma-separated value (.csv), netCDF (.nc), and ArcGIS shape (.shp) formats through the NWA regional climatology webpage mentioned above. Other NCEI regional climatologies completed to date, can be found at NCEI regional climatology webpage NCEI Regional Ocean Climatologies. A pilot study was published by Seidov *et al.* (2015) which shows an example of using these new high-resolution regional climatologies in oceanographic research. There are several published scientific publications specifically targeting the NWA region, with focus on the Gulf Stream and surrounding areas (Seidov *et al.*, 2017; Seidov *et al.*, 2018; Seidov *et al.*, 2019a; b; Seidov *et al.*, 2021).

It is important to note that the high-resolution monthly temperature and salinity data coverage on the one-tenth-degree grid have more gaps than seasonal and annual fields computed from the monthly fields. In general, all high-resolution analyzed fields should be reviewed carefully before using them in mission-critical applications. It is especially important when working with the high-resolution monthly fields. Users are advised to review the data distribution and statistical mean maps before deciding whether to use the high-resolution analyzed temperature and salinity fields or their climatological means. Moreover, the monthly maps of objectively analyzed data on one-tenth-degree grid may show some possibly spurious eddy-like irregularities

in some regions due to interpolation and plotting artefacts combined. Although such cases are very rare, a more careful review of the fields with such occurrences is needed before using analyzed variables in research or applications.

Displaying only monthly fields that are shallower than 1500 m requires more explanation. Indeed, we do not know how deep the seasonal signal can penetrate the ocean. Were the mixing in the ocean only limited to the upper mixed layer with turbulent diffusion below that layer, the seasonal signal would be confined to the upper several hundred meters. In most of the ocean volume this would probably be true, but in regions of strong upwelling and convection, especially seasonal deep convection in high latitudes, seasonal variability can penetrate quite deep, which is seen in the analyzed fields. On the other hand, the scarcity of data below 1500 m depth makes any seasonal analysis questionable, at the very least. It may soon improve, as Argo floats, which reaches 2000 m depth, become more abundant, but for the time being the data below 1500 m in the NWARC v2 area are still noticeably scarcer compared to the upper ocean. Thus, a reasonable solution was to show decadal monthly fields above 1500 m only. Although seasonal fields are shown below 1500 m, they should be considered rather cautiously. In contrast, the aggregated annual fields computed by averaging all data can be deemed as more reliable than "seasonal" fields, as more data are available and additional smoothing is applied while averaging over the four seasons. This issue needs a more careful consideration in future research to determine how variability in the deep ocean is to be treated.

11. DISCUSSION

The most important feature of the new NWA fine resolution regional climatology is the six-decade-long timespan, which makes NWARC v2 a useful tool for assessing ocean long-term variability. Notably, although spatial and temporal changes can be assessed to some degree using the WOA18 on the quarter-degree grid, many features of the NWA regional ocean climate dynamics cannot be evaluated properly because the spatial scales of the processes in this region cannot be adequately represented on the grid coarser than one-tenth of a degree (or better, if possible).

In fact, one can refer to NWARC, or any RC with 0.1°x0.1° or better resolution, as an "eddy-resolving" regional climatology as it can reveal the cumulative effect of the mesoscale processes in the climatological fields (Seidov *et al.*, 2018; Seidov *et al.*, 2019a). The basis for this lies in the fundamental structure of the ocean currents and related hydrological fields. As mentioned previously, a parameter called the Rossby baroclinic radius of deformation, ***R***, e.g., (Gill, 1982), provides the condition for resolving oceanic mesoscale motion in numerical models or in ocean data mapping. The grid size needed for resolving mesoscale motion must be shorter than ***R***. In the middle latitudes, ***R*** is ~30–40 km, which is roughly the latitudinal dimensions of one to two grid cells with 1/4°x1/4° grid resolution (~25 km spatial resolution in latitude). A hydrographic front ~50-70 km wide, which is approximately the width the Gulf Stream, can be relatively well resolved on a 1/10°x1/10° grid (~10 km spatial resolution in latitude and ~8 km in longitude in mid-latitudes), and would be just barely "permitted" on the 1/4°x1/4°grid. Such a front would be completely unresolved at coarser resolutions (e.g., 1°x1° with scale of ~100 km in latitude).

Seidov et al. (2019) argue that the seasonal signal carries the superimposed repetitive mesoscale signals and thus decadal climatologies—monthly, seasonal, and annual—reflect the cumulative effect of mesoscale dynamics on mapping of the large-scale regional ocean climate state and variability. This will be discussed further in the text when the mesoscale features of the NWARC v2 are compared to some available satellite observations of sea surface temperature.

Figures 11 and 12, showing winter temperature and salinity for the 2005-2017, provide the examples of difference in climatologies with different resolutions. In general, an important advantage gained by using fine spatial resolution, obvious in Figures 9 and 10, is that the Gulf Stream and Gulf Stream Extension features are more coherent in one-tenth degree analysis than in the quarter-degree one, and of course far more coherent than in the analysis on the one-degree grid. All frontal zones are noticeably narrower on the finer grid and far better reflect the cumulative effects of mesoscale dynamics characteristic for this area.

One feature of the fine-resolution maps that really stands out in Figures 11 and 12 is the Gulf Stream structure in the southwest corner of the domain. The jet is highly coherent and parallel to the continental shelf break in the one-tenth of a degree case (Figures 9c and 10c), while on the

quarter-degree grid this pronounced jet character is completely lost. The slope water north of the Gulf Stream Extension is also better resolved on the finest-resolution grid. The Gulf Stream jet looks very narrow, as it should be. It is about half of the width of the jet emerging in the quarter-degree maps and is up to three to four times narrower if compared to one-degree plots where the Gulf Stream completely loses its narrow jet nature.

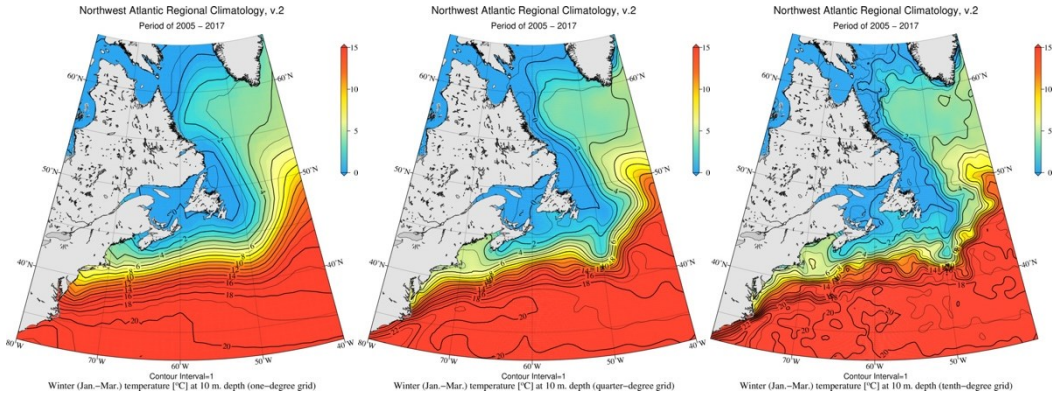

a) **b)** **c)**

Figure 11. Winter objectively analyzed temperature averaged over the period of 2005-2017 at 10 m depth in three analyses on: (a) one-degree, (b) quarter-degree, and (c) one-tenth-degree grids.

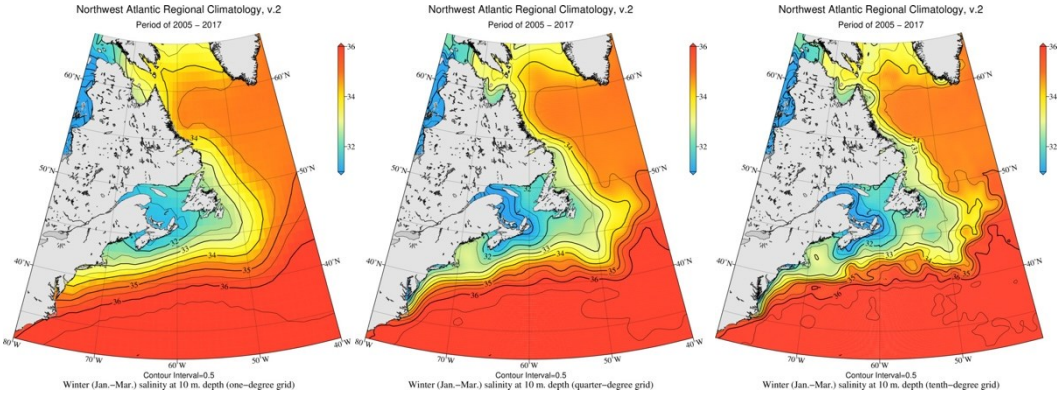

a) **b)** **c)**

Figure 12. Winter objectively analyzed salinity averaged over the period of 2005-2017 at 10 m depth in three analyses on: (a) one-degree, (b) quarter-degree, and (c) one-tenth-degree grids.

Employing one-tenth degree resolution allows locating the correct position of the jet separation from the shelf at Cape Hatteras (see the discussion in (Holt *et al.*, 2014)) and to depict a more complex and realistic MLTZ. A clearer representation of the cold and fresh water carried

by the Labrador Current south of Nova Scotia along the New England shelf with one-tenth-degree resolution is obvious when compared to one-degree or quarter-degree resolutions. The Slope Water Current looks better aligned in its recirculation path to form the Gulf Stream "northern wall" (Frankignoul *et al.*, 2001; Joyce *et al.*, 2013).

Salinity in Figure 12c shows the frontal features like the thermal front (to form the density front of the same quality) shown in Figure 11c and it is well pronounced and narrow, as usually seen in advanced eddy-resolving numerical models.

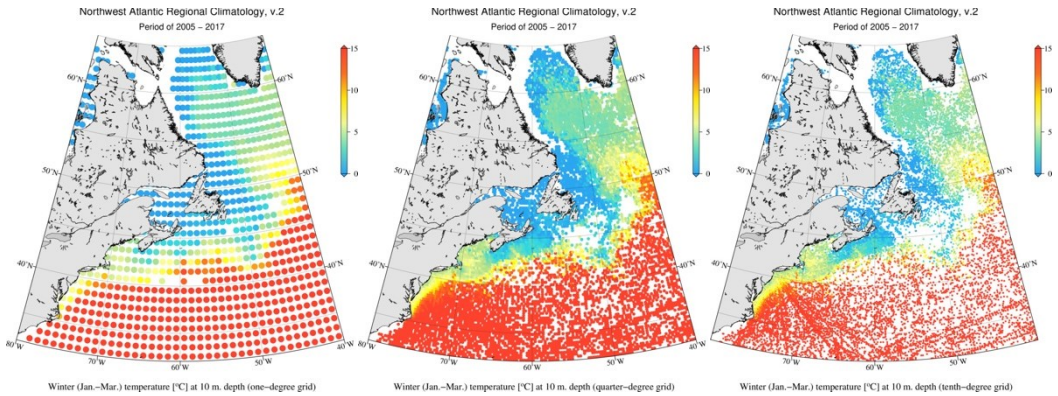

a) **b)** **c)**

Figure 13. Winter objectively analyzed temperature averaged over the years 2005-2017 at 10 m depth in three analyses on: (a) one-degree, (b) quarter-degree, and (c) one-tenth-degree grids.

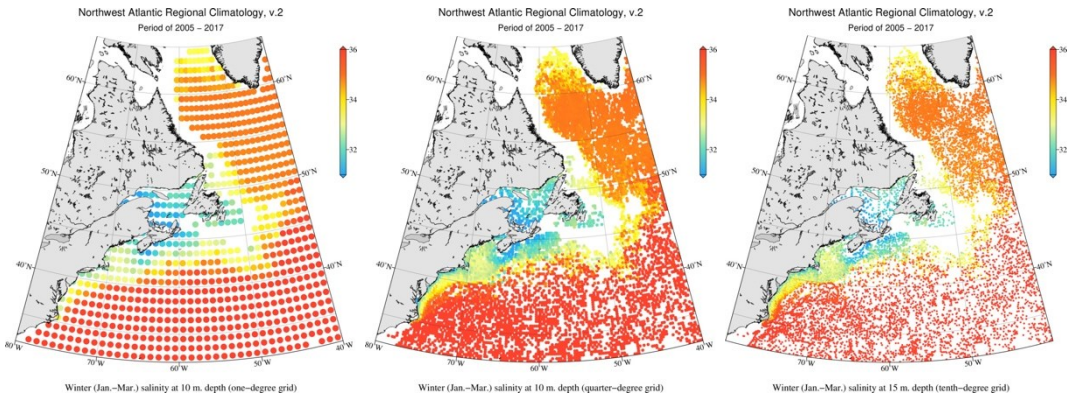

a) **b)** **c)**

Figure 14. Winter statistical mean salinity averaged over the years 2005-2017 at 10 m depth in three analyses on: (a) one-degree, (b) quarter-degree, and (c) one-tenth-degree grids.

The temperature and salinity shown in Figures 9 and 10 were computed using the objective analysis technique, which, while indisputably powerful, has its own weaknesses, as have all

interpolation techniques; in particular, it may generate artificial features if the gaps between data filled cells are too numerous. As the NWA is a region rather densely covered by observations, the simple statistical mean can be used to assess the quality of the objectively analyzed fields in this domain (Figures 13 and 14).

The standard error of the mean is noticeably reduced in many places on the finer grid, as can be expected. Indeed, the standard error for the three resolutions (the same time interval and depth as in all other maps above) shows substantial improvement at the finer grids, especially in the Gulf Stream area from Florida Strait up to Nova Scotia and in the Labrador Sea (Figure 15).

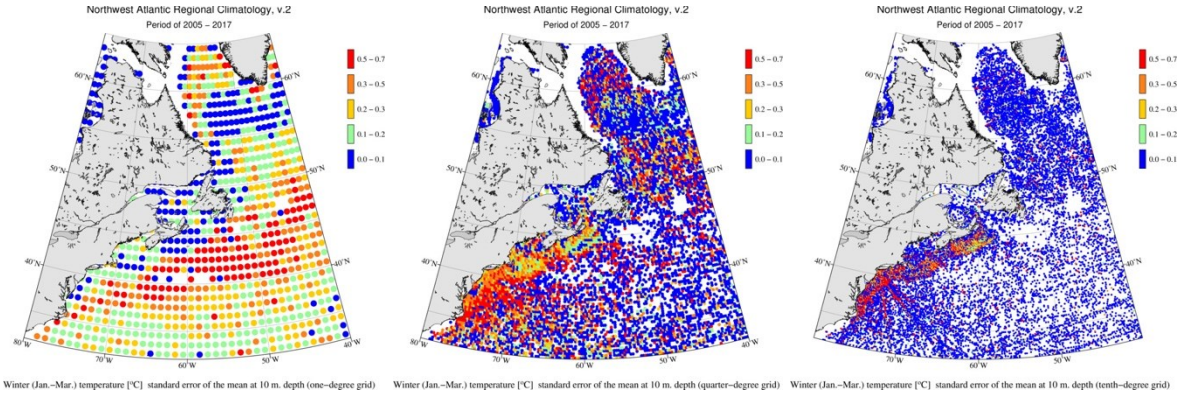

a) **b)** **c)**

Figure 15. Standard error of temperature at 10 m depth for winter averaged over the period of 2005-2012 in three analyses on: (a) one-degree, (b) quarter-degree, and (c) one-tenth-degree grids.

Another important feature of the high-resolution climatological fields that are far more pronounced seasonality of the Gulf Stream jet revealed in hydrological fields shown on Figures 16, 17, and 18.

There is a fundamental issue about the observation-based decadal climatologies regarding the "cumulative" mesoscale effects, or the mesoscale activity averaged over a decadal timespan. The seasonal variability is stronger than the mesoscale variability, as is confirmed when reviewing the annual climatologies for any decade. Figure 16 shows the annual temperature climatologies for three decades. Temperature at 10 m depth for winter and January for the same three decades is shown in Figures 17 and 18. The jet and its meandering are strongest in January if compared to the winter or annual fields (and much stronger compared to warmer seasons and months).

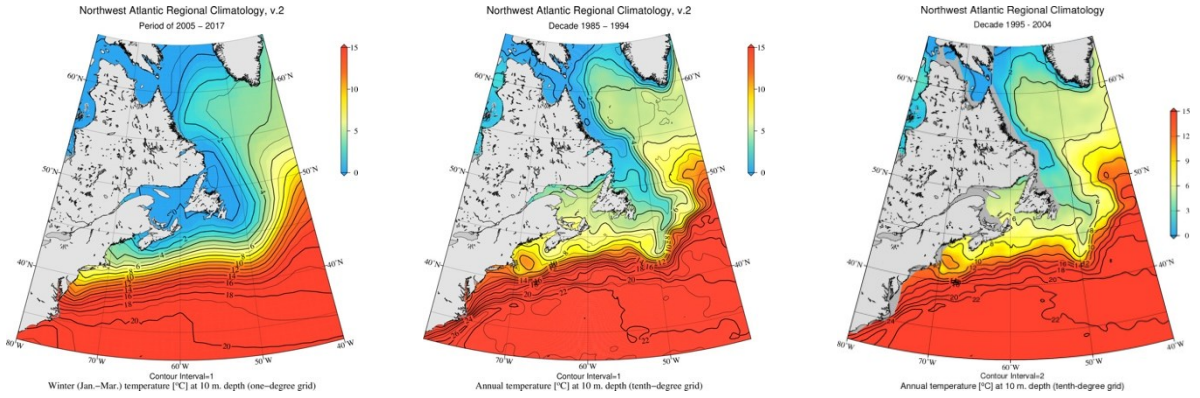

a) **b)** **c)**

Figure 16. Annual mean temperature at 10 m depth for three decades: (a) 1965-1974, (b) 1985-1994, and (c) 2005-2017 on one-tenth-degree grid.

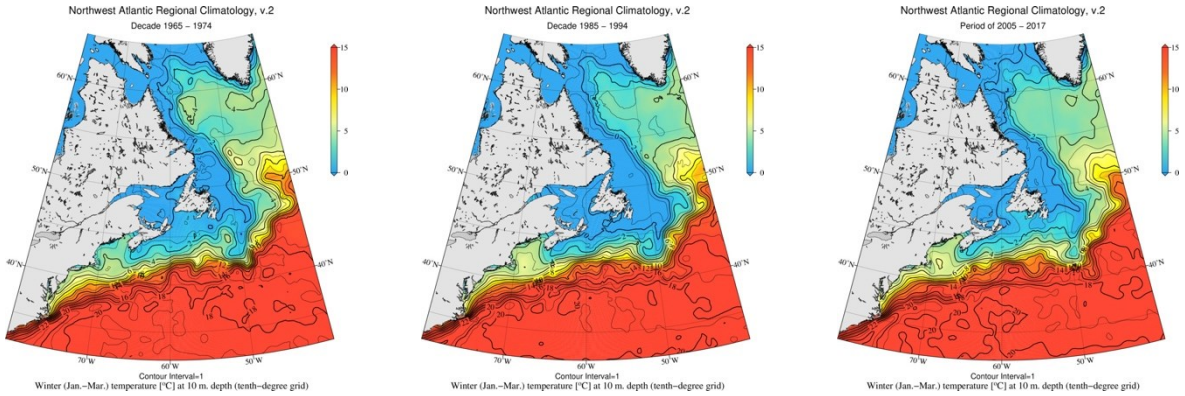

a) **b)** **c)**

Figure 17. Winter mean temperature at 10 m depth for three decades: (a) 1965-1974, (b) 1985-1994, and (c) 2005-2017 on one-tenth-degree grid.

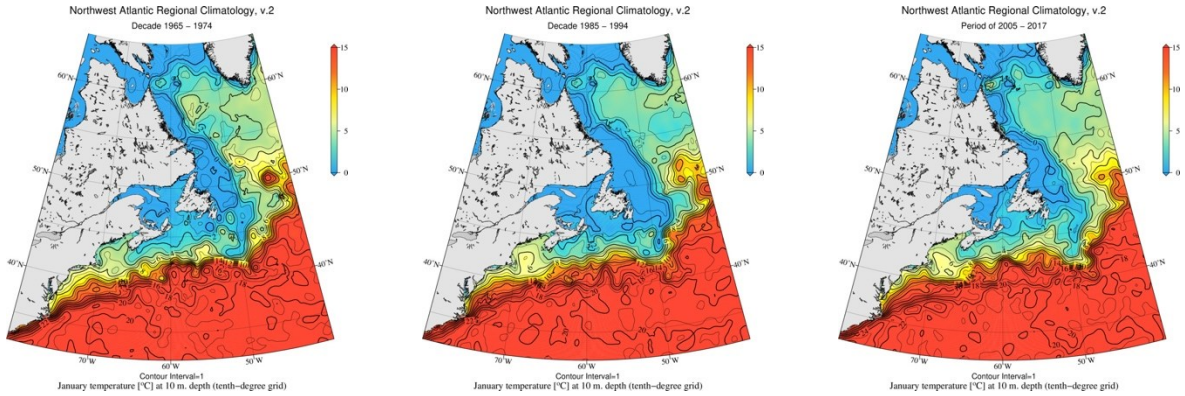

a) **b)** **c)**

Figure 18. January mean temperature at 10 m depth for three decades: (a) 1965-1974, (b) 1985-1994, and (c) 2005-2017 on one-tenth-degree grid.

The striking feature in Figures 17 and 18, where the climatological winter and climatological January are shown, is the repetitiveness of major mesoscale features in

climatological seasonal and monthly fields. The fact that very similar mesoscale patterns (meanders and Gulf Stream eddies) are seen in all decades implies that there is a cumulative effect of mesoscale activities overlaying a clear seasonal signal. The seasonal signal is obviously stronger than the signal generated by mesoscale eddies, but the eddy-type motion is amplified by the seasonal signal. Indeed, repetitive mesoscale patterns superimposed over the seasonal variability must repeat statistically not only every year in each decade, but also every year in all decades since 1955. On the other hand, as the seasonal maps show, there are also distinctive differences between the seasons in the 1965-64, 1985-94, and 2005-2017 sequence indicating stochastic nature of mesoscale variability superimposed over the carrying seasonal signal with multi-decadal quasi-periodical cyclicity.

Snapshots of sea surface temperature from both satellite imagery and eddy-resolving numerical simulations (see an example in Figure 3) disclose a strong structural resemblance between the NWA monthly observations-based high-resolution regional climatologies and the remotely sensed and numerically simulated ones. Importantly, the monthly temperatures averaged over a decade show an aggregated realization of the Gulf Stream and mesoscale eddies. There was no guarantee that averaging over a long period, such as a decade, would yield such resemblance (years and decades compared to week and months as a characteristic time scale of the mesoscale variability). Nonetheless, there is a line of thinking that mesoscale variability is interlocked with seasonal cyclicity and that there is a great deal of repetitiveness of specific patterns surrounding unstable jet currents, especially the Gulf Stream and Gulf Stream Extension, e.g., (Kelly *et al.*, 2010).

As discussed above, the spatial resolution of a regional climatology, either in climate reconstructions using observed data or in climate modeling, is the key for better understanding the role of regional dynamics in such critical areas such as the Gulf Stream, Kuroshio, etc. Moreover, it is becoming obvious that long-term climate forecasting is impossible without detailed knowledge of decadal variability (Siqueira and Kirtman, 2016). Even atmosphere-only sensitivity experiments have demonstrated the impact of increasing horizontal resolution and have indicated that seasonal variability of the Gulf Stream has a substantial impact on the troposphere dynamics (Minobe *et al.*, 2008). In their numerical simulations, Minobe *et al.* (2008) showed that an atmospheric general circulation model with about 50 km resolution responds quite noticeably to

the observed sharpness of the Gulf Stream front, and they showed that the Gulf Stream affects the entire troposphere. In fact, a poorly resolved Gulf Stream presents a structural problem for atmospheric climate models preventing them from capturing observed decadal climate variability in the North Atlantic (Siqueira and Kirtman, 2016). That is, the sharpness, internal dynamics, and cumulative effect of mesoscale eddies and other transients on decadal scale may become critical for the success of long-term climate forecasting. The key to understanding why decadal climatologies are so important is that they emphasize the repetitiveness or statistical periodicity of the major elements of mesoscale processes in the Gulf Stream system.

Figure 19 reproduces two monthly-averaged satellite sea-surface temperature snapshots, four years apart, in March of 2003 and in 2007, in the Gulf Stream region (Kelly *et al.*, 2010).

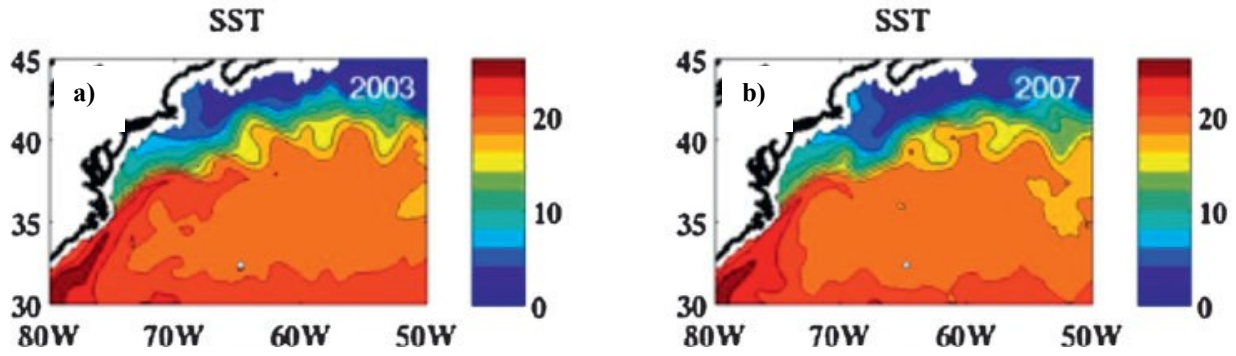

Figure 19. March averages of SST for (a) 2003 and (b) 2007. SST fields are from the Remote Sensing Systems on a 0.258° grid spatial resolution from Kelly *et al.* (2010).

As can be seen in Figure 19, although the patterns are not exactly the same (and they would not and should not be expected to be, of course), they are surprisingly similar implying the quasi-stationary character of mesoscale variability in the Gulf Stream jet vicinity. In previous paragraphs, we discussed the striking repetitiveness of the mesoscale temperature patterns, like what is shown in Figure 19. When the NWARC v1 became available (Seidov *et al.*, 2016), the idea of retaining some of repetitive mesoscale variability in the observed ocean climatology was put forth (Seidov *et al.*, 2018; Seidov *et al.*, 2019a). The following is a brief outline of the premise that the mesoscale variability can at least partly be present in the monthly ocean climatologies.

To verify the hypothesis that the seasonal signal carries superimposed repetitive mesoscale features that can be seen in averaged seasonal climatologies, the seawater temperature in the NWA region was compared with the sea surface temperature (SST) from satellite observations (Seidov *et al.*, 2018).

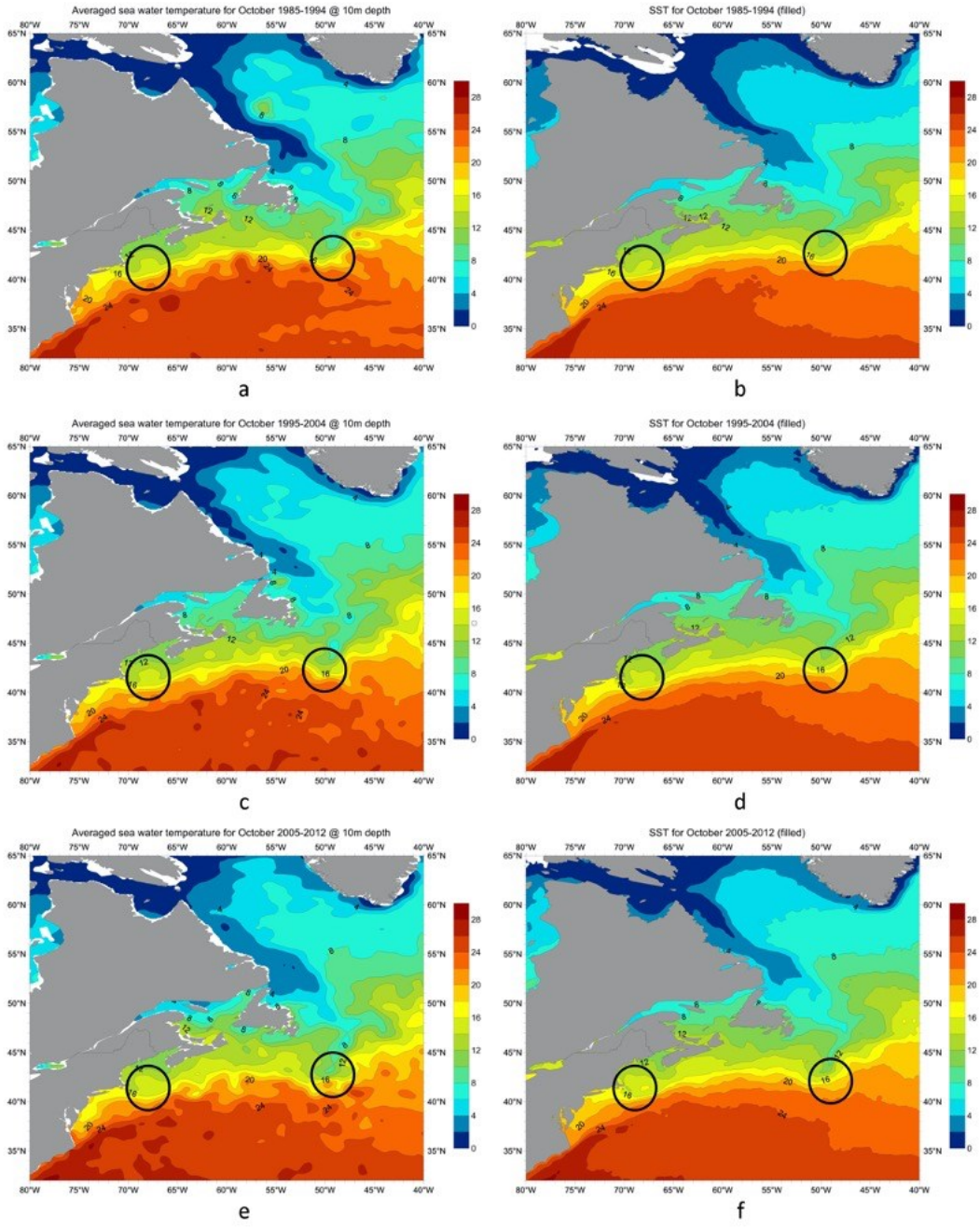

Figure 20. Climatological October seawater temperature from (left) NWARC v1 at 10m depth and (right) sea surface temperature (SST) from satellite observations for the decades 1985-1994, 1995-2004, and 2005-2012. The satellite SST maps were created from CoRTADv5 (Casey *et al.*, 2015). Examples of repetitive filaments in the Gulf Stream Extension area are denoted by the black circles. Reproduced from (Seidov *et al.*, 2018 with permission from American Meteorological Society).

This SST was extracted from the Coral Reef Temperature Anomaly Database version 5 (CoRTADv5). The CoRTADv5 SST arrays are derived from the Advanced Very High-Resolution Radiometer (AVHRR) Pathfinder v5.2 data and are available for the time span between 1982 and

2012 (Casey *et al.*, 2015). The approximate spatial resolution of the data is 4 km (~1/20th of a degree at mid-latitudes) with one-week temporal resolution.

To make the satellite-derived SST comparable with the NWARC v1 near-surface in situ temperature, the weekly satellite SST data were averaged into monthly fields for every year over the 1982-2012-time period. Then, to compute the decadal satellite SST climatology, we took each month of the decades 1985-1994, 1995-2004, and 2005-2012 and averaged them within each decade.

High-resolution regional climatologies may be especially useful for comparison between results of numerical simulations and observed data. Therefore, we include a part of the previous analysis to show an example of the model-data comparison. The following discussion is based on the NWARC v1 (Seidov *et al.*, 2016), but everything fully applies to NWARC v2. As the NWARC v1 became available, it was tempting to compare the in situ climatologies with an eddy-resolving model. Therefore, to further substantiate the hypothesis that repetitive mesoscale variability can be revealed in the observed high-resolution ocean climatology, the extractions from NWARC v1 were compared with those from eddy-resolving numerical simulations. The model employed for the data-model comparison is the Nucleus for European Modelling of the Ocean (NEMO) modeling system (Madec, 2008) with a global 1/12th degree grid, which is close to NWARC v2 one-tenth of a degree resolution. The NEMO is a state-of-the-art modeling framework for oceanographic research, operational oceanography seasonal forecasting, and climate studies. (More details about the NEMO modeling can be found at the NEMO ocean model website).

The simulations were adopted from the set of eight experiments described in detail in the MJM8 set of model experiments (Molines *et al.*, 2014). These simulations are a part of an extensive international DRAKKAR project using ORCA12 model configuration described, for example, in (Molines *et al.*, 2014) and (Treguier *et al.*, 2014). DRAKKAR is a scientific and technical coordination between several European teams. The output from MJM88 NEMO experiments (courtesy of Jean-Marc Molines of University of Grenoble, France) covers ocean temperature, salinity, velocity, and several other variables for 55 years, from 1958 to 2012 at 1/12-deg resolution for every 5 days. That is, the computed fields were averaged over each pentad for the entire 55-year interval) (Molines *et al.*, 2014).

All model-generated data were averaged for each month of the selected decades. Then seasons were computed as the average of the climatological months, whereas the climatological annual mean was computed as the average of four seasons. The output from the NEMO model was re-plotted in the NWA domain to facilitate easier visual comparison between NWARC v2 and model's results.

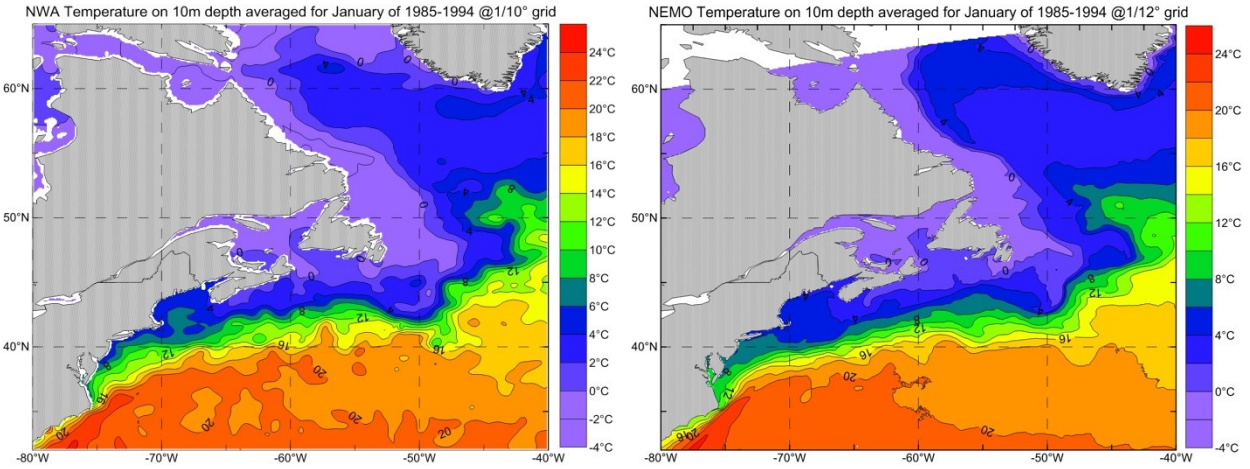

Figure 21. January temperature at 10 m depth from (a) NWARC v2 and (b) the NEMO numerical experiments for the decade 1985-1994 (see the website NEMO ocean model).

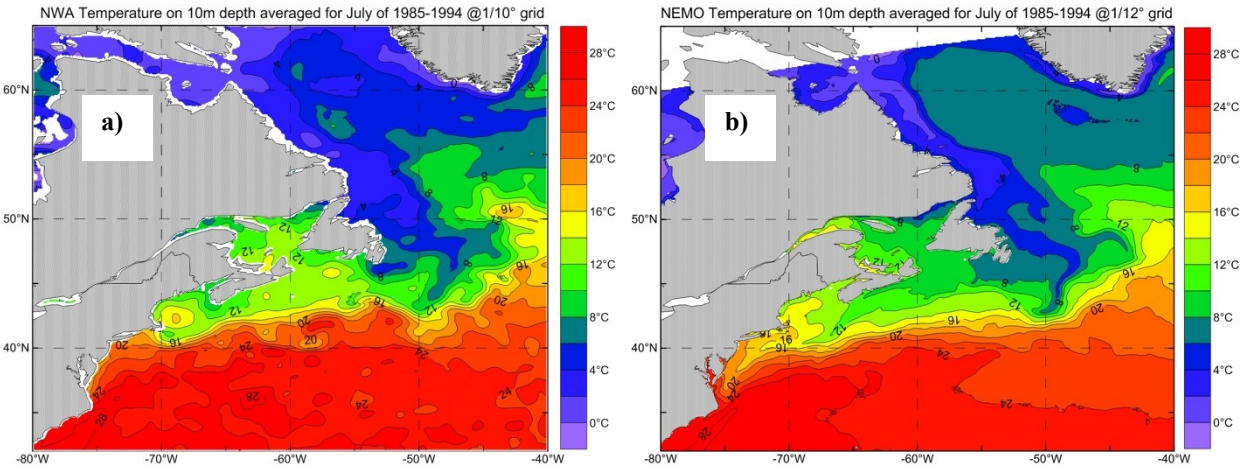

Figure 22. July temperature at 10 m depth from (a) NWARC v2 and (b) the NEMO numerical experiments for the decade 1985-1994 (see the website NEMO ocean model).

Figure 21 shows the observation-based temperature at 10m depth averaged over climatological January of 1985-1994 from NWARC v2 (a) and the MJM88 NEMO simulation for

the same decade (b), while Figure 22 depicts a similar comparison between NWARC v2 (a) and MJM88 NEMO (b) for July of 1985-1994.

Although we do not expect identical patterns, there are clear similarities between the patterns of observed and modeled climatological months. Moreover, NEMO simulations are on 1/12th-degree grid, so some additional inconsistencies because of slight grid resolution differences could be a possibility. Nonetheless, similarities between the maps are quite evident. For example, both climatological Januarys show strong advection along the coast toward the separation point off Cape Hatteras, with a strong Slope Water Current, while July's temperature shows far warmer water at the Gulf Stream separation point. The series of meanders and eddy-like formations is seen in approximately the same areas and appears to be of similar or at least comparable amplitude. For instance, there is a very pronounced meander of cold water in the MLTZ, in the northeast part of the region in both observed and modelled climatologies. In general, the cumulative impact of mesoscale motion on large-scale circulation dynamics is apparently of the same nature in observed and modelled climatologies.

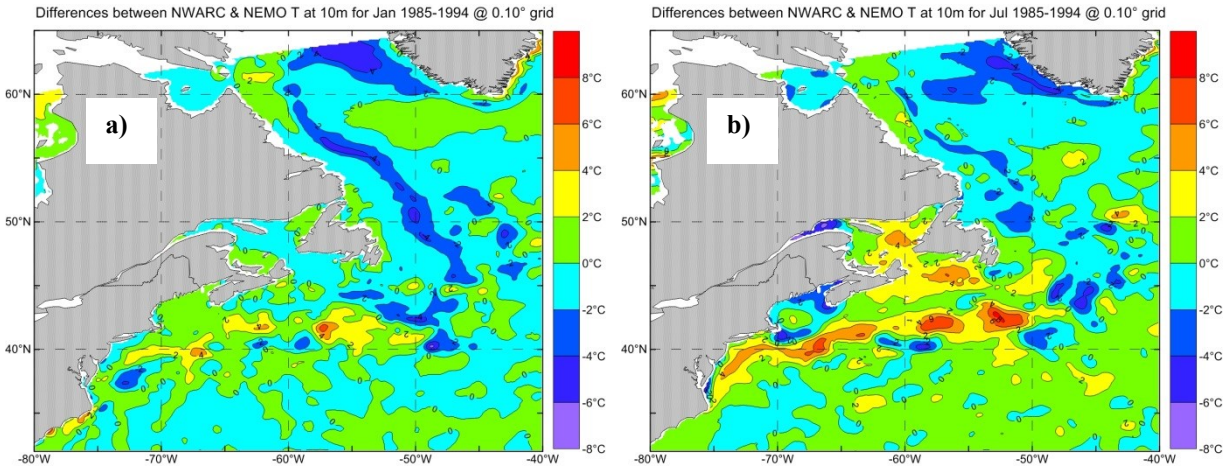

Figure 23. Differences between decadal mean temperature at 10 m depth from NWARC v2 and NEMO model in January (a) and July (b) for the decade of 1985-1994 (see Figures 19 and 20, and text).

To support the arguments about similarities between observed and modeled climatologies, Figures 23 and 24 illustrate the differences and the root mean square (RMS) of differences, which shows the magnitude of deviations between fields of the observed and modeled decadal temperature at 10m depth for the decade of 1985-1994.

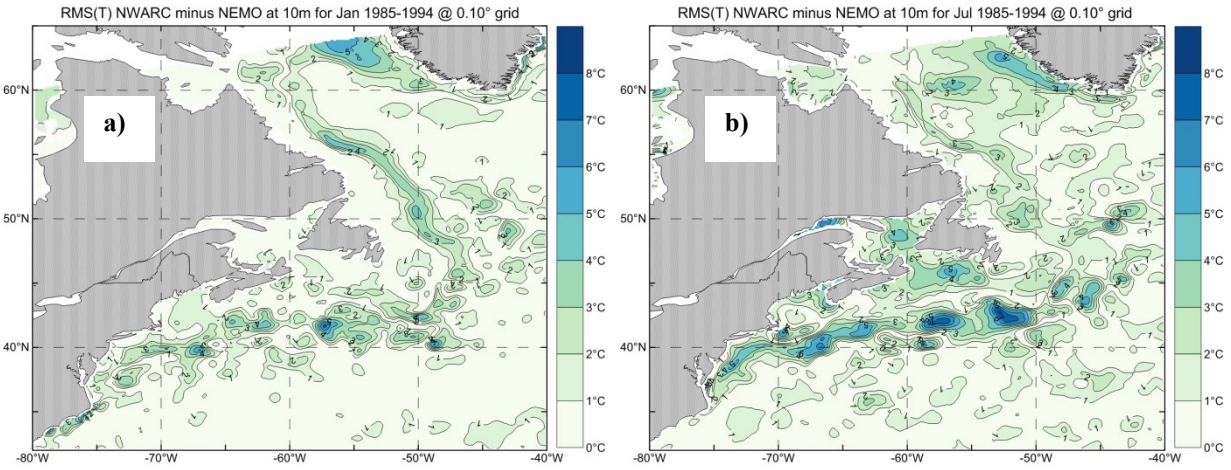

Figure 24. RMS of differences between observed and modeled decadal temperature at 10 m depths in January (a) and July (b) for the decade of 1985-1994 (see Figures 19 and 20, and text).

In the highly variable zone of unstable jet, RMS of differences between observed and model data is higher than in other regions. However, it is surprisingly low almost everywhere else, including the Gulf Stream core zone for summer and winter months.

High-resolution ocean climatologies, like NWARC, may have many uses in climate forecast models, but the most important one may be the use of sea surface salinity (SSS) for correcting for long-term drift in model simulations of ocean circulation, which is critical for ocean climate simulations and especially in long-term climate forecasts. As was found in early simulation experiments with coupled ocean-atmosphere models, the freshwater fluxes in such models must be pre-computed using observed SSS to avoid the so-called climate drift, which is an artefact caused by poorly-resolved freshwater fluxes across the ocean surface in practically any coupled ocean-atmosphere model (Bryan, 1998; Huang *et al.*, 2015; Manabe and Stouffer, 1988). After more than a quarter of a century since such a drift was identified in (Manabe and Stouffer, 1988), forecast models use the method of restoring the model to the observed SSS for suppressing such artificial climate drift. Moreover, it turned out that the SSS from earlier editions of WOA were not sufficient as they are too smooth because of infilling the gaps and objective interpolation on a coarse-resolution grid, e.g., (Molines *et al.*, 2014). However, Molines et al. (2014) used older one-degree fields. New WOA18, with quarter-degree resolution may already provide sufficiently detailed SSS for such numerical simulations, while for the regions covered by high-resolution climatologies, the best would be using one-tenth-degree grid whenever possible. Providing high-

resolution sea surface salinity on quarter- and one-tenth-degree grids with well-resolved frontal structures may be critical for improving long-term ocean climate forecasts.

12. SUMMARY

We have presented the description and results of the Northwest Atlantic Regional Climatology project aimed at generating objectively analyzed historical ocean temperature and salinity data fields. The effort of creating NWARC v1 Atlas (Seidov *et al.*, 2016) yielded several new research papers, e.g., (Seidov *et al.*, 2017; Seidov *et al.*, 2018; Seidov *et al.*, 2019a; b; Seidov *et al.*, 2021). The new updated version of NWARC—NWARC v2 —that includes new observations as well as rescued from earlier cruises, is now available. The advantages of high-resolution regional climatologies along with an updated discussion of how such climatologies may align with remote sensing of sea surface and with eddy-resolving ocean numerical modeling were also presented. It is argued now that a high-resolution regional climatology like the NWARC v2 may be viewed as eddy-resolving in situ climatology (Seidov *et al.*, 2019a).

Currently, only temperature and salinity decadal climatologies have been created with one-tenth-degree spatial resolution. These climatologies were compiled to provide investigators from various branches of oceanography, climatology, fisheries, and other related disciplines with oceanographic foundations that define long-term ocean climate change inferred from observations. Coarse-resolution maps and data for other important oceanographic parameters can be assessed at the NCEI Ocean Climate Laboratory website; see also (Garcia *et al.*, 2019a; b).

When computing anomalies from a standard climatology, it is important that the synoptic field be smoothed to the same extent as the climatology, to prevent generation of spurious anomalies simply through differences in smoothing. However, on finer resolution grids mesoscale eddies are directly resolved and the remaining mesoscale background probably represents a cumulative effect of mesoscale dynamics rather than a noise generated by objective analysis. The advantage of a high-resolution grid becomes obvious as the shorter radii of influence used in the objective analysis leads to less diffusive fields in the frontal zones, which bears sharp gradients, especially in the coastal regions. In a sense, the finer-resolution analysis suits the same goal as reducing grid sizes in numerical models.

The high-resolution regional climatologies narrows the gaps between observations and modeling and allow meaningful data-model comparisons in critical regions, such as the Northwest Atlantic Ocean. Moreover, in a new class of long-term ocean climate forecast modeling, the analyzed regional climatologies can be used for restoring the simulated fields to the observed ones (especially sea surface salinity) and thus prevent the climate drift effect that plagues even the most advanced climate models.

As in all WOA editions and regional climatologies, the main goal is to create objectively analyzed fields and data sets that can be used as a "black box" in applications. The new and significant feature we now offer are six high-resolution decadal climatologies that can be used in assessing "true" ocean climate change backed up by aggregated historical oceanographic in situ observations. Naturally, some quality control procedures used are somewhat subjective. Moreover, monthly decadal fields are less reliable because of more data gaps than in seasonal or annual fields, so some mesoscale features could still be affected by artefacts caused by lack of data. However, seasonal, and annual fields are very well supported by data, especially in recent decades.

Disclaimer: Users of the NWARC, and all other high-resolution regional climatologies for that matter, are advised to inspect very carefully the data distributions, statistical means, standard errors, etc., before deciding to what extent they can rely on the objectively analyzed data and maps in their mission-critical research and application developments. For users who wish to make their own choices, all data used in WOA18 and NWARC v2 analyses, both at standard and observed depth levels, are available at World Ocean Database.

In very rare cases, some maps at some depths in monthly fields in the NWARC, especially in earlier decades, may show some peculiarities that may be due to non-representativeness of data and have not yet been flagged by manual quality control described in the text. Although we have made all reasonable efforts to eliminate as many of these features as possible by flagging the data that generate such features, some could still be undetected and remain unflagged. Some may eventually turn out not to be artefacts, but rather represents real features. In such rare cases, we are not capable yet to describe and explain them in any meaningful way due to lack of data. In any of such cases, which are very few, users are advised to be extremely cautious and make all possible efforts to recognize where the analyzed fields are sufficiently supported by observations by using

the supplied additional statistical fields, such as simple statistics, number of available observations, standard errors, etc.

13. FUTURE WORK

Our analyses will be updated when justified by newly available observations. As more data are received and archived in WOD, there may be a ground to produce improved higher resolution regional climatologies for temperature and salinity and perhaps for some other essential oceanographic variables. The NWARC v2 will be further updated in concert with the next update of WOA when it became available.

14. REFERENCES

Allison, E. H.*, and Co-authors* (2009), Vulnerability of national economies to the impacts of climate change on fisheries, *Fish and Fisheries*, *10*(2), 173-196, doi:10.1111/j.1467-2979.2008.00310.x.

Antonov, J. I., D. Seidov, T. P. Boyer, R. A. Locarnini, A. V. Mishonov, and H. E. Garcia (2010), World Ocean Atlas 2009, Volume 2: Salinity, in *NOAA Atlas NESDIS*, edited by S. Levitus, p. 184, U.S. Government Printing Office, Washington, D.C.

Arguez, A., and R. S. Vose (2011), The Definition of the Standard WMO Climate Normal: The Key to Deriving Alternative Climate Normals, *Bulletin of the American Meteorological Society*, *92*(6), 699-704, doi:10.1175/2010bams2955.1.

Barange, M., and R. P. Harris (2010), *Marine ecosystems and global change*, 412 pp., Oxford University Press Oxford.

Barnes, S. L. (1964), A Technique for Maximizing Details in Numerical Weather Map Analysis, *Journal of Applied Meteorology*, *3*(4), 396-409, doi:10.1175/1520-0450(1964)003<0396:atfmdi>2.0.co;2.

Barnes, S. L. (1973), Mesoscale objective map analysis using weighted time series observations, in *NOAA Technical Memorandum ERL NSSL 62*, edited, Wash. D.C.

Barnes, S. L. (1994), Applications of the Barnes Objective Analysis Scheme. Part III: Tuning for Minimum Error, *Journal of Atmospheric and Oceanic Technology*, *11*(6), 1459-1479, doi:doi:10.1175/1520-0426(1994)011.

Barrier, N., J. Deshayes, A.-M. Treguier, and C. Cassou (2015), Heat budget in the North Atlantic subpolar gyre: impacts of atmospheric weather regimes on the 1995 warming event, *Progress in Oceanography*, *130*(0), 75-90, doi:http://dx.doi.org/10.1016/j.pocean.2014.10.001.

Bernard, B.*, and Co-authors* (2006), Impact of partial steps and momentum advection schemes in a global ocean circulation model at eddy-permitting resolution, *Ocean Dynamics*, *56*(5), 543-567, doi:10.1007/s10236-006-0082-1.

Blanchard, J. L.*, and Co-authors* (2012), Potential consequences of climate change for primary

production and fish production in large marine ecosystems, *Philosophical Transactions of the Royal Society of London B: Biological Sciences*, *367*(1605), 2979-2989, doi:10.1098/rstb.2012.0231.
Blunden, J., and T. Boyer (2021), State of the Climate in 2020, *Bulletin of the American Meteorological Society*, *102*(8), S1-S475, doi:10.1175/2021BAMSStateoftheClimate.1.
Bower, A.*, and Co-authors* (2019), Lagrangian Views of the Pathways of the Atlantic Meridional Overturning Circulation, *Journal of Geophysical Research: Oceans*, *124*(8), 5313-5335, doi:https://doi.org/10.1029/2019JC015014.
Bower, A. S., H. T. Rossby, and J. L. Lillibridge (1985), The Gulf Stream—Barrier or Blender?, *J. Phys. Oceanogr.*, *15*(1), 24-32, doi:10.1175/1520-0485(1985)015<0024:tgsob>2.0.co;2.
Boyer, T., S. Levitus, H. Garcia, R. A. Locarnini, C. Stephens, and J. Antonov (2005), Objective analyses of annual, seasonal, and monthly temperature and salinity for the World Ocean on a 0.25° grid, *International Journal of Climatology*, *25*(7), 931-945, doi:10.1002/joc.1173.
Boyer, T. P.*, and Co-authors* (2013), World Ocean Database 2013*Rep.*, 209 pp, U.S. Government Printing Office, Washington, D.C.
Boyer, T. P.*, and Co-authors* (2018a), World Ocean Database 2018, NOAA Atlas NESDIS 87 (A.V. Mishonov, Tech. Editor) *Rep.*, NOAA/NESDIS, Silver Spring, MD.
Boyer, T. P.*, and Co-authors* (2018b), World Ocean Atlas 2018 NOAA*Rep.*
Brander, K. (2010), Impacts of climate change on fisheries, *Journal of Marine Systems*, *79*(3–4), 389-402, doi:http://dx.doi.org/10.1016/j.jmarsys.2008.12.015.
Broecker, W. (1991), The great ocean conveyor, *Oceanography*, *1*, 79-89.
Bryan, F. O. (1998), Climate drift in a multicentury integration of the NCAR climate system model, *J. Climate*, *11*(6), 1455-1471.
Bryan, K. (1986), Poleward buoyancy transport in the ocean and mesoscale eddies, *J. Phys. Oceanogr.*, *16*(5), 927-933.
Bryden, H. L., H. R. Longworth, and S. A. Cunningham (2005), Slowing of the Atlantic meridional overturning circulation at 25°N, *Nature*, *438*(7068), 655-657.
Buckley, M. W., and J. Marshall (2016), Observations, inferences, and mechanisms of Atlantic Meridional Overturning Circulation variability: A review, *Rev. Geophys.*, *54*, 5-63, doi:10.1002/2015RG000493.
Caesar, L., S. Rahmstorf, A. Robinson, G. Feulner, and V. Saba (2018), Observed fingerprint of a weakening Atlantic Ocean overturning circulation, *Nature*, *556*(7700), 191-196, doi:10.1038/s41586-018-0006-5.
Casey, K. S., E. R. Selig, D. Zhang, K. Saha, A. Krishnan, and E. McMichael (2015), The Coral Reef Temperature Anomaly Database (CoRTAD) Version 5 - Global, 4 km Sea Surface Temperature and Related Thermal Stress Metrics for 1982-2012 (NCEI Accession 0126774). edited by N. N. C. f. E. Information, NOAA National Centers for Environmental Information, doi:10.7289/V5CZ3545.
Chao, Y., A. Gangopadhyay, F. O. Bryan, and W. R. Holland (1996), Modeling the Gulf Stream System: How far from reality?, *Geophys. Res. Lett.*, *23*(22), 3155-3158, doi:10.1029/96GL03003.
Charney, J. G. (1971), Geostrophic Turbulence, *J. Atmos. Sci.*, *28*, 1087-1095, doi:http://dx.doi.org/10.1175/1520-0469(1971)028%3C1087:GT%3E2.0.CO;2.
Chelton, D. B., M. G. Schlax, and R. M. Samelson (2011), Global observations of nonlinear

mesoscale eddies, *Progress in Oceanography*, *91*(2), 167-216, doi:http://dx.doi.org/10.1016/j.pocean.2011.01.002.
Cornillon, P., and R. Watts (1987), Satellite Thermal Infrared and Inverted Echo Sounder Determinations of the Gulf Stream Northern Edge, *Journal of Atmospheric and Oceanic Technology*, *4*(4), 712-723, doi:10.1175/1520-0426(1987)004<0712:Stiaie>2.0.Co;2.
Cox, M. (1975), A baroclinic numerical model of the world ocean: Preliminary results, in *Numerical Models of Ocean Circulation*, edited, pp. 107-120, National Academy of Sciences, Washington, DC.
Cunningham, S. A.*, and Co-authors* (2007), Temporal Variability of the Atlantic Meridional Overturning Circulation at 26.5°N, *Science*, *317*(5840), 935-938, doi:10.1126/science.1141304.
Dai, A., A. Hu, G. A. Meehl, W. M. Washington, and W. G. Strand (2005), Atlantic Thermohaline Circulation in a Coupled General Circulation Model: Unforced Variations versus Forced Changes, *J. Climate*, *18*(16), 3270-3293, doi:doi:10.1175/JCLI3481.1.
Drinkwater, K. F. (2005), The response of Atlantic cod (Gadus morhua) to future climate change, *ICES J. Mar. Sci.*, *62*(7), 1327-1337, doi:10.1016/j.icesjms.2005.05.015.
Drinkwater, K. F., F. Mueter, K. D. Friedland, M. Taylor, G. L. Hunt Jr, J. Hare, and W. Melle (2009), Recent climate forcing and physical oceanographic changes in Northern Hemisphere regions: A review and comparison of four marine ecosystems, *Progress in Oceanography*, *81*(1–4), 10-28, doi:10.1016/j.pocean.2009.04.003.
Drinkwater, K. F.*, and Co-authors* (2013a), The Response of Marine Ecosystems to Climate Variability Associated with the North Atlantic Oscillation, in *The North Atlantic Oscillation: Climatic Significance and Environmental Impact*, edited by Y. K. J. W. Hurrell, G. Ottersen and M. Visbeck, pp. 211-234, American Geophysical Union, Washington, D.C., doi:10.1029/134GM10.
Drinkwater, K. F., E. Colbourne, H. Loeng, S. Sundby, and T. Kristiansen (2013b), Comparison of the atmospheric forcing and oceanographic responses between the Labrador Sea and the Norwegian and Barents seas, *Progress in Oceanography*, *114*(0), 11-25, doi:http://dx.doi.org/10.1016/j.pocean.2013.03.007.
Edwards, M., G. Beaugrand, L. Kléparski, P. Hélaouët, and P. C. Reid (2022), Climate variability and multi-decadal diatom abundance in the Northeast Atlantic, *Communications Earth & Environment*, *3*(1), 162, doi:10.1038/s43247-022-00492-9.
Frajka-Williams, E., P. B. Rhines, and C. C. Eriksen (2009), Physical controls and mesoscale variability in the Labrador Sea spring phytoplankton bloom observed by Seaglider, *Deep Sea Research Part I: Oceanographic Research Papers*, *56*(12), 2144-2161, doi:http://dx.doi.org/10.1016/j.dsr.2009.07.008.
Frajka-Williams, E.*, and Co-authors* (2019), Atlantic Meridional Overturning Circulation: Observed Transport and Variability, *Frontiers in Marine Science*, *6*(260), doi:10.3389/fmars.2019.00260.
Frankignoul, C., G. d. Coëtlogon, T. M. Joyce, and S. Dong (2001), Gulf Stream Variability and Ocean–Atmosphere Interactions, *J. Phys. Oceanogr.*, *31*(12), 3516-3529, doi:doi:10.1175/1520-0485(2002)031<3516:GSVAOA>2.0.CO;2.
Fuglister, F. C. (1963), Gulf stream '60, *Progress in Oceanography*, *1*, 265-373, doi:http://dx.doi.org/10.1016/0079-6611(63)90007-7.
Garcia, H.*, and Co-authors* (2019a), World ocean atlas 2018. Vol. 4: Dissolved inorganic nutrients (phosphate, nitrate and nitrate+ nitrite, silicate).

Garcia, H.*, and Co-authors* (2019b), World Ocean Atlas 2018, Volume 3: Dissolved Oxygen, Apparent Oxygen Utilization, and Dissolved Oxygen Saturation.
Gill, A. E. (1982), *Atmosphere-ocean Dynamics*, 662 pp., Academic Press, New York.
Gonçalves Neto, A., J. A. Langan, and J. B. Palter (2021), Changes in the Gulf Stream preceded rapid warming of the Northwest Atlantic Shelf, *Communications Earth & Environment*, *2*(1), 74, doi:10.1038/s43247-021-00143-5.
Gordon, A. L. (1986), Interocean exchange of thermocline water, *J. Geophys. Res.*, *91*, 5037-5046.
Gould, J.*, and Co-authors* (2004), Argo profiling floats bring new era of in situ ocean observations, *Eos, Transactions American Geophysical Union*, *85*(19), 185-191, doi:10.1029/2004EO190002.
Gula, J., M. J. Molemaker, and J. C. McWilliams (2014), Submesoscale Cold Filaments in the Gulf Stream, *J. Phys. Oceanogr.*, *44*(10), 2617-2643, doi:10.1175/JPO-D-14-0029.1.
Guttman, N. B. (1989), Statistical Descriptors of Climate, *Bulletin of the American Meteorological Society*, *70*(6), 602-607, doi:doi:10.1175/1520-0477(1989)070<0602:SDOC>2.0.CO;2.
Harning, D. J., A. E. Jennings, D. Köseoğlu, S. T. Belt, Á. Geirsdóttir, and J. Sepúlveda (2021), Response of biological productivity to North Atlantic marine front migration during the Holocene, *Clim. Past*, *17*(1), 379-396, doi:10.5194/cp-17-379-2021.
Hogg, N. G., R. S. Pickart, R. M. Hendry, and W. J. Smethie Jr (1986), The northern recirculation gyre of the Gulf Stream, *Deep Sea Research Part A. Oceanographic Research Papers*, *33*(9), 1139-1165, doi:http://dx.doi.org/10.1016/0198-0149(86)90017-8.
Hogg, N. G., and W. E. Johns (1995), Western boundary currents, *Rev. Geophys.*, *33*(S2), 1311-1334, doi:10.1029/95RG00491.
Holt, J.*, and Co-authors* (2009), Modelling the global coastal ocean, *Philosophical Transactions of the Royal Society of London A: Mathematical, Physical and Engineering Sciences*, *367*(1890), 939-951, doi:10.1098/rsta.2008.0210.
Holt, J.*, and Co-authors* (2014), Challenges in integrative approaches to modelling the marine ecosystems of the North Atlantic: Physics to fish and coasts to ocean, *Progress in Oceanography*, *129, Part B*(0), 285-313, doi:http://dx.doi.org/10.1016/j.pocean.2014.04.024.
Huang, B.*, and Co-authors* (2015), Climate drift of AMOC, North Atlantic salinity and arctic sea ice in CFSv2 decadal predictions, *Clim. Dyn.*, *44*(1), 559-583, doi:10.1007/s00382-014-2395-y.
Hurlburt, H. E.*, and Co-authors* (2008), Eddy-Resolving Global Ocean Prediction, in *Ocean Modeling in an Eddying Regime*, edited by M. W. Hecht and H. Hasumi, pp. 353-381, American Geophysical Union, Washiongton, D.C., doi:10.1029/177GM21.
Isachsen, P. E., S. R. Sørlie, C. Mauritzen, C. Lydersen, P. Dodd, and K. M. Kovacs (2014), Upper-ocean hydrography of the Nordic Seas during the International Polar Year (2007–2008) as observed by instrumented seals and Argo floats, *Deep Sea Research Part I: Oceanographic Research Papers*, *93*(0), 41-59, doi:http://dx.doi.org/10.1016/j.dsr.2014.06.012.
Iselin, C. (1936), A study of the circulation of the western North Atlantic, in *Papers in Physical Oceanography and Meteorology*, edited, p. 101.
Iselin, C., and F. C. Fuglister (1948), Some recent developments in the study of the Gulf Stream,

J. Mar. Res., *7*, 317-329.
Jackett, D. R., and T. J. Mcdougall (1995), Minimal Adjustment of Hydrographic Profiles to Achieve Static Stability, *Journal of Atmospheric and Oceanic Technology*, *12*(2), 381-389, doi:doi:10.1175/1520-0426(1995)012<0381:MAOHPT>2.0.CO;2.
Jackson, L. C., A. Biastoch, M. W. Buckley, D. G. Desbruyères, E. Frajka-Williams, B. Moat, and J. Robson (2022), The evolution of the North Atlantic Meridional Overturning Circulation since 1980, *Nature Reviews Earth & Environment*, doi:10.1038/s43017-022-00263-2.
Jennings, S., and K. Brander (2010), Predicting the effects of climate change on marine communities and the consequences for fisheries, *Journal of Marine Systems*, *79*(3–4), 418-426, doi:http://dx.doi.org/10.1016/j.jmarsys.2008.12.016.
Johnson, G. C.*, and Co-authors* (2022), Argo—Two Decades: Global Oceanography, Revolutionized, *Annual Review of Marine Science*, *14*(1), 379-403, doi:10.1146/annurev-marine-022521-102008.
Joyce, T. M., and R. Zhang (2010), On the Path of the Gulf Stream and the Atlantic Meridional Overturning Circulation, *J. Climate*, *23*(11), 3146-3154, doi:10.1175/2010JCLI3310.1.
Joyce, T. M., L. N. Thomas, W. K. Dewar, and J. B. Girton (2013), Eighteen Degree Water formation within the Gulf Stream during CLIMODE, *Deep Sea Research Part II: Topical Studies in Oceanography*, *91*, 1-10, doi:http://dx.doi.org/10.1016/j.dsr2.2013.02.019.
Kamenkovich, V. M., M. N. Koshlyakov, and A. S. Monin (1986), *Synoptic eddies in the ocean*, 433 pp., Reidel, Dordrecht, holland.
Kamykowski, D. (2014), Twentieth century Atlantic meridional overturning circulation as an indicator of global ocean multidecadal variability: influences on sea level anomalies and small pelagic fishery synchronies, *ICES Journal of Marine Science: Journal du Conseil*, *71*(3), 455-468, doi:10.1093/icesjms/fst165.
Kelly, K. A., R. J. Small, R. M. Samelson, B. Qiu, T. M. Joyce, Y.-O. Kwon, and M. F. Cronin (2010), Western Boundary Currents and Frontal Air–Sea Interaction: Gulf Stream and Kuroshio Extension, *J. Climate*, *23*(21), 5644-5667, doi:doi:10.1175/2010JCLI3346.1.
Klatt, O., O. Boebel, and E. Fahrbach (2007), A Profiling Float's Sense of Ice, *Journal of Atmospheric and Oceanic Technology*, *24*(7), 1301-1308, doi:doi:10.1175/JTECH2026.1.
Klymak, J. M.*, and Co-authors* (2016), Submesoscale streamers exchange water on the north wall of the Gulf Stream, *Geophys. Res. Lett.*, *43*(3), 1226-1233, doi:10.1002/2015GL067152.
Lee, T., and P. Cornillon (1995), Temporal variation of meandering intensity and domain-wide lateral oscillations of the Gulf Stream, *Journal of Geophysical Research: Oceans*, *100*(C7), 13603-13613, doi:doi:10.1029/95JC01219.
Lehodey, P.*, and Co-authors* (2006), Climate Variability, Fish, and Fisheries, *J. Climate*, *19*(20), 5009-5030, doi:10.1175/jcli3898.1.
Leterme, S. C., and R. D. Pingree (2008), The Gulf Stream, rings and North Atlantic eddy structures from remote sensing (Altimeter and SeaWiFS), *Journal of Marine Systems*, *69*(3–4), 177-190, doi:http://dx.doi.org/10.1016/j.jmarsys.2005.11.022.
Levitus, S. (1982), *Climatological Atlas of the World Ocean. NOAA Professional Paper 13*, 173 pp., U.S. Gov. Printing Office, Princeton, N.J.
Levitus, S., J. I. Antonov, T. P. Boyer, and C. Stephens (2000), Warming of the World Ocean, *Science*, *287*, 2225-2229.
Levitus, S., J. I. Antonov, T. P. Boyer, R. A. Locarnini, H. E. Garcia, and A. V. Mishonov

(2009), Global ocean heat content 1955-2008 in light of recently revealed instrumentation problems, *Geophys. Res. Lett.*, *36*, L07608, doi:07610.01029/02008GL037155.
Levitus, S.*, and Co-authors* (2012), World ocean heat content and thermosteric sea level change (0–2000 m), 1955–2010, *Geophys. Res. Lett.*, *39*(10), L10603, doi:10610.11029/12012GL051106, doi:10.1029/2012gl051106.
Livezey, R. E., K. Y. Vinnikov, M. M. Timofeyeva, R. Tinker, and H. M. v. d. Dool (2007), Estimation and Extrapolation of Climate Normals and Climatic Trends, *Journal of Applied Meteorology and Climatology*, *46*(11), 1759-1776, doi:doi:10.1175/2007JAMC1666.1.
Locarnini, R. A., A. V. Mishonov, J. I. Antonov, T. P. Boyer, and H. E. Garcia (2010), World Ocean Atlas 2009, Volume 1: Temperature., in *NOAA Atlas NESDIS*, edited by S. Levitus, p. 184, U.S. Government Printing Office, Washington, D.C.
Locarnini, R. A.*, and Co-authors* (2018), World Ocean Atlas 2018, Volume 1: Temperature (A. Mishonov Technical Ed.); NOAA Atlas NESDIS 81, 52 pp.*Rep.*, 52 pp, NOAA/NESDIS, Silver Spring, MD.
Lozier, M. S.*, and Co-authors* (2017), Overturning in the Subpolar North Atlantic Program: A New International Ocean Observing System, *Bulletin of the American Meteorological Society*, *98*(4), 737-752, doi:10.1175/bams-d-16-0057.1.
Lynn, R. J., and J. L. Reid (1968), Characteristics and circulation of deep and abyssal waters, *Deep Sea Research and Oceanographic Abstracts*, *15*(5), 577-598, doi:http://dx.doi.org/10.1016/0011-7471(68)90064-8.
Madec, G. (2008), NEMO ocean general circulation model reference manual, in *Internal Report*, edited, LODYC/IPSL Paris.
Mahajan, S., R. Zhang, T. L. Delworth, S. Zhang, A. J. Rosati, and Y.-S. Chang (2011), Predicting Atlantic meridional overturning circulation (AMOC) variations using subsurface and surface fingerprints, *Deep Sea Research Part II: Topical Studies in Oceanography*, *58*(17–18), 1895-1903, doi:http://dx.doi.org/10.1016/j.dsr2.2010.10.067.
Maltrud, M. E., and J. L. McClean (2005), An eddy resolving global 1/10° ocean simulation, *Ocean Modelling*, *8*(1-2), 31-54.
Manabe, S., and R. J. Stouffer (1988), Two stable equilibria of a coupled ocean-atmosphere model, *J. Climate*, *1*, 841-866.
Mann, K. H., and J. R. Lazier (2013), *Dynamics of marine ecosystems: biological-physical interactions in the oceans*, John Wiley & Sons.
Marzocchi, A., J. J. M. Hirschi, N. P. Holliday, S. A. Cunningham, A. T. Blaker, and A. C. Coward (2015), The North Atlantic subpolar circulation in an eddy-resolving global ocean model, *Journal of Marine Systems*, *142*, 126-143, doi:http://dx.doi.org/10.1016/j.jmarsys.2014.10.007.
Mesick, S., Z. Wang, A. Mishonov, T. Boyer, and H. m. Zhang (2020), Incorporating Discrete Unmanned Maritime System Data Collections Into NCEI Synthesized Data Products, paper presented at Global Oceans 2020: Singapore – U.S. Gulf Coast, 5-30 Oct. 2020.
Meyer, D. (2016), Glider Technology for Ocean Observations: A Review, *Ocean Sci. Discuss.*, *2016*, 1-26, doi:10.5194/os-2016-40.
Minobe, S., A. Kuwano-Yoshida, N. Komori, S.-P. Xie, and R. J. Small (2008), Influence of the Gulf Stream on the troposphere, *Nature*, *452*(7184), 206-209, doi:http://www.nature.com/nature/journal/v452/n7184/suppinfo/nature06690_S1.html.
Molines, J., B. Barnier, T. Penduff, A. Treguier, and J. Le Sommer (2014), ORCA12. L46

climatological and interannual simulations forced with DFS4. 4: GJM02 and MJM88. Drakkar Group Experiment Rep*Rep.*, GDRI-DRAKKAR-2014-03-19, 50 pp.[Available online at http://www.drakkar-ocean.eu/publications/reports/orca12_reference_experiments_2014.].

Monin, A. S. (1986), *An introduction into the theory of climate*, 261 pp., D. Reidel Publishing Company, Dordrecht.

Munk, W. H. (1950), On the wind-driven ocean circulation, *Journal of Meteorology*, *7*(2), 79-93.

Nakamura, M., and T. Kagimoto (2006), Transient wave activity and its fluxes in the North Atlantic Ocean simulated by a global eddy-resolving model, *Dynamics of Atmospheres and Oceans*, *41*(1), 60-84.

Nye, J. (2010), *Climate Change and its effects on Ecosystems, Habitats and Biota: State of the Gulf of Maine Report*.

Nye, J. A*., and Co-authors* (2014), Ecosystem effects of the Atlantic Multidecadal Oscillation, *Journal of Marine Systems*, *133*(0), 103-116, doi:http://dx.doi.org/10.1016/j.jmarsys.2013.02.006.

Overland, J. E., J. Alheit, A. Bakun, J. W. Hurrell, D. L. Mackas, and A. J. Miller (2010), Climate controls on marine ecosystems and fish populations, *Journal of Marine Systems*, *79*(3–4), 305-315, doi:http://dx.doi.org/10.1016/j.jmarsys.2008.12.009.

Owens, W. B., N. Zilberman, K. S. Johnson, H. Claustre, M. Scanderbeg, S. Wijffels, and T. Suga (2022), OneArgo: A New Paradigm for Observing the Global Ocean, *Marine Technology Society Journal*, *56*(3), 84-90.

Peña-Molino, B., and T. M. Joyce (2008), Variability in the Slope Water and its relation to the Gulf Stream path, *Geophys. Res. Lett.*, *35*(3), L03606, doi:10.1029/2007GL032183.

Puerta, P*., and Co-authors* (2020), Influence of Water Masses on the Biodiversity and Biogeography of Deep-Sea Benthic Ecosystems in the North Atlantic, *Frontiers in Marine Science*, *7*(239), doi:10.3389/fmars.2020.00239.

Rayner, D*., and Co-authors* (2011), Monitoring the Atlantic meridional overturning circulation, *Deep Sea Research Part II: Topical Studies in Oceanography*, *58*(17–18), 1744-1753, doi:http://dx.doi.org/10.1016/j.dsr2.2010.10.056.

Rhines, P. B. (2001), Mesoscale Eddies, in *Encyclopedia of Ocean Sciences*, edited by J. H. Steele, pp. 1717-1730, Academic Press, Oxford, doi:http://dx.doi.org/10.1006/rwos.2001.0143.

Richardson, P. L. (2001), Florida Current, Gulf Stream, and Labrador Current, in *Encyclopedia of Ocean Sciences (Second Edition)*, edited by J. H. Steele, pp. 554-563, Academic Press, Oxford, doi:https://doi.org/10.1016/B978-012374473-9.00357-X.

Riser, S. C*., and Co-authors* (2016), Fifteen years of ocean observations with the global Argo array, *Nature Clim. Change*, *6*(2), 145-153, doi:10.1038/nclimate2872.

Roemmich, D., and W. B. Owens (2002), The ARGO project: Global ocean observations for understanding and prediction of climate variability, *Oceanography*, *13*(2), 45– 50.

Roemmich, D., and Argo-Steering-Team (2009), Argo: The challange of continuing 10 years of progress, *Oceanography*, *22*(3), 27-35.

Rossby, T., C. Flagg, and K. Donohue (2010), On the variability of Gulf Stream transport from seasonal to decadal timescales, *J. Mar. Res.*, *68*(3-1), 503-522, doi:10.1357/002224010794657128.

Rossby, T., C. N. Flagg, K. Donohue, A. Sanchez-Franks, and J. Lillibridge (2014), On the long-term stability of Gulf Stream transport based on 20 years of direct measurements,

Geophys. Res. Lett., *41*(1), 2013GL058636, doi:10.1002/2013GL058636.
Rudnick, D. L. (2016), Ocean Research Enabled by Underwater Gliders, *Annual Review of Marine Science*, *8*(1), 519-541, doi:10.1146/annurev-marine-122414-033913.
Sarmiento, J. L.*, and Co-authors* (2004), Response of ocean ecosystems to climate warming, *Glob. Biogeochem. Cycles*, *18*(GB3003), 23.
Schmittner, A. (2005), Decline of the marine ecosystem caused by a reduction in the Atlantic overturning circulation, *Nature*, *434*, 628-633.
Schmitz, W. J., Jr., and M. S. McCartney (1993), On the North Atlantic circulation, *Rev. Geophys.*, *31*, 29-49.
Schollaert, S. E., T. Rossby, and J. A. Yoder (2004), Gulf Stream cross-frontal exchange: possible mechanisms to explain interannual variations in phytoplankton chlorophyll in the Slope Sea during the SeaWiFS years, *Deep Sea Research Part II: Topical Studies in Oceanography*, *51*(1–3), 173-188, doi:http://dx.doi.org/10.1016/j.dsr2.2003.07.017.
Seidov, D. (1989), Synergetics of the ocean circulation, in *Mesoscale/synoptic coherent structures in geophysicai turbulence*, edited by J. C. J. Nihoul and B. M. Jamart, p. 21, Elsevier, Amsterdam.
Seidov, D.*, and Co-authors* (2015), Oceanography north of 60°N from World Ocean Database, *Progress in Oceanography*, *132*, 153-173, doi:http://dx.doi.org/10.1016/j.pocean.2014.02.003.
Seidov, D., O. K. Baranova, T. Boyer, S. L. Cross, A. V. Mishonov, and A. R. Parsons (2016), Northwest Atlantic Regional Ocean Climatology (A.V. Mishonov, Technical Ed.), NOAA Atlas NESDIS 80, 56 pp.*Rep.*, 56 pp, NOAA/NESDIS, Silver Spring, MD.
Seidov, D., A. Mishonov, J. Reagan, and R. Parsons (2017), Multidecadal variability and climate shift in the North Atlantic Ocean, *Geophys. Res. Lett.*, *44*(10), 4985-4993, doi:10.1002/2017GL073644.
Seidov, D., A. Mishonov, J. Reagan, O. Baranova, S. Cross, and R. Parsons (2018), Regional Climatology of the Northwest Atlantic Ocean: High-Resolution Mapping of Ocean Structure and Change, *Bulletin of the American Meteorological Society*, *99*(10), 2129-2138, doi:10.1175/bams-d-17-0205.1.
Seidov, D., A. Mishonov, J. Reagan, and R. Parsons (2019a), Eddy-Resolving In Situ Ocean Climatologies of Temperature and Salinity in the Northwest Atlantic Ocean, *Journal of Geophysical Research: Oceans*, *124*(1), 41-58, doi:doi:10.1029/2018JC014548.
Seidov, D., A. Mishonov, J. Reagan, and R. Parsons (2019b), Resilience of the Gulf Stream path on decadal and longer timescales, *Scientific Reports*, *9*(1), 11549, doi:10.1038/s41598-019-48011-9.
Seidov, D., A. Mishonov, and R. Parsons (2021), Recent warming and decadal variability of Gulf of Maine and Slope Water, *Limnology and Oceanography*, *66*, 3472-3488, doi:https://doi.org/10.1002/lno.11892.
Seidov, D. G., and A. D. Maruskevich (1992), Order and chaos in ocean current dynamics:numerical experiment, *Dynamics of Atmospheres and Oceans*, *16*, 405-434.
Seip K.L, Grøn Ø, and W. H. (2019), The North Atlantic Oscillations: Cycle Times for the NAO, the AMO and the AMOC, *Climate*, *7*(3), doi:https://doi.org/10.3390/cli7030043.
Semtner, A. J., and R. M. Chervin (1988), A simulation of the global ocean circultion with resolved eddies, *J. Geophys. Res.*, *93*, 15502-15522.
Semtner, A. J., and R. M. Chervin (1993), Including eddies in global ocean models, *Eos, Transactions American Geophysical Union*, *74*(5), 59-59, doi:10.1029/93EO00215.

Semtner, A. J. (1995), Modeling Ocean Circulation, *Science*, *269*(5229), 1379-1385, doi:10.1126/science.269.5229.1379.
Shackell, N. L., D. Rickard, and C. Stortini (2014), Thermal Habitat Index of Many Northwest Atlantic Temperate Species Stays Neutral under Warming Projected for 2030 but Changes Radically by 2060, *PLOS*, *9*(3), doi:10.1371/journal.pone.0090662, doi:10.1371/journal.pone.0090662.
Sherman, K., I. Belkin, K. D. Friedland, and J. O'Reilly (2013), Changing states of North Atlantic large marine ecosystems, *Environmental Development*, *7*(0), 46-58, doi:http://dx.doi.org/10.1016/j.envdev.2013.05.004.
Siqueira, L., and B. P. Kirtman (2016), Atlantic near-term climate variability and the role of a resolved Gulf Stream, *Geophys. Res. Lett.*, *43*(8), 3964-3972, doi:10.1002/2016GL068694.
Skjoldal, H. R., and K. Sherman (2002), *Large marine ecosystems of the North Atlantic: changing states and sustainability*, Elsevier.
Smeed, D. A.*, and Co-authors* (2014), Observed decline of the Atlantic Meridional Overturning Circulation 2004 to 2012, *Ocean Sci.*, *10*(5), 29-38, doi:doi:10.5194/os-10-29-2014.
Smeed, D. A.*, and Co-authors* (2018), The North Atlantic Ocean Is in a State of Reduced Overturning, *Geophys. Res. Lett.*, *45*(3), 1527-1533, doi:10.1002/2017GL076350.
Srokosz, M.*, and Co-authors* (2012), Past, Present, and Future Changes in the Atlantic Meridional Overturning Circulation, *Bulletin of the American Meteorological Society*, *93*(11), 1663-1676, doi:10.1175/bams-d-11-00151.1.
Stenseth, N. (2004), *Marine Ecosystems and Climate Variation: The North Atlantic. A Comparative Perspective*, OUP Oxford.
Steven, R. J., D. Roemmich, N. Zilberman, S. C. Riser, K. S. Johnson, G. C. Johnson, and S. R. Piotrowicz (2017), The Argo Program: Present and Future, *Oceanography*, *30*(2), 18-28, doi:https://doi.org/10.5670/oceanog.2017.213.
Stommel, H. (1948), The westward intensification of the wind-driven ocean circulation, *Trans. Amer. Geophys. Union*, *29*, 202-230.
Stommel, H. (1958), *The Gulf Stream*, 202 pp., University of California, Berkeley, California.
Taylor, A. H. (1996), North–south shifts of the Gulf Stream: Ocean-atmosphere interactions in the North Atlantic, *International Journal of Climatology*, *16*(5), 559-583, doi:10.1002/(SICI)1097-0088(199605)16:5<559::AID-JOC26>3.0.CO;2-Z.
Taylor, A. H., and J. A. Stephens (1998), The North Atlantic Oscillation and the latitude of the Gulf Stream, *Tellus A*, *50*(1), 134-142, doi:10.1034/j.1600-0870.1998.00010.x.
Taylor, J. R. (1997), *An Introduction to Error Analysis*, 2 ed., University Science Books, Sausalito, CA.
Thomson, R. E., and W. J. Emery (2014), *Data analysis methods in physical oceanography, 3d Edition*, Third Edition ed., 716 pp., Elsevier, Amsterdam, The Netherlands.
Toole, J. M., R. A. Krishfield, M.-L. Timmermans, and A. Proshutinsky (2011), The Ice-Tethered Profiler: Argo of the Arctic, *Oceanography*, *24*(3), 126-135, doi:http://dx.doi.org/10.5670/oceanog.2011.64.
Treguier, A. M.*, and Co-authors* (2014), Meridional transport of salt in the global ocean from an eddy-resolving model, *Ocean Sci.*, *10*(2), 243-255, doi:10.5194/os-10-243-2014.
WMO (2011), *World Meteorological Organization: Guide to Climatological Practices*, 2011 Edition ed., 117 pp., WMO, Geneva, Switzerland.
Wong, A. P. S., and S. C. Riser (2011), Profiling Float Observations of the Upper Ocean under

Sea Ice off the Wilkes Land Coast of Antarctica, *J. Phys. Oceanogr.*, *41*(6), 1102-1115, doi:doi:10.1175/2011JPO4516.1.

Wong, A. P. S., and S. C. Riser (2013), Modified shelf water on the continental slope north of Mac Robertson Land, East Antarctica, *Geophys. Res. Lett.*, *40*(23), 6186-6190, doi:10.1002/2013GL058125.

Worthington, E. L., B. I. Moat, D. A. Smeed, J. V. Mecking, R. Marsh, and G. D. McCarthy (2021), A 30-year reconstruction of the Atlantic meridional overturning circulation shows no decline, *Ocean Sci.*, *17*(1), 285-299, doi:10.5194/os-17-285-2021.

Worthington, L. V. (1976), *On the North Atlantic circulation*, 110 pp., Johns Hopkins University Press, Baltimore.

Wunsch, C. (1978), The North Atlantic general circulation west of 50°W determined by inverse methods, *Rev. Geophys.*, *16*(4), 583-620, doi:10.1029/RG016i004p00583.

Yashayaev, I., D. Seidov, and E. Demirov (2015), A new collective view of oceanography of the Arctic and North Atlantic basins, *Progress in Oceanography*, *132*, 1-21, doi:http://dx.doi.org/10.1016/j.pocean.2014.12.012.

Zhongming, Z., L. Linong, Y. Xiaona, Z. Wangqiang, and L. Wei (2021), AR6 climate change 2021: The physical science basis.

Zweng, M. M., T. P. Boyer, O. K. Baranova, J. R. Reagan, D. Seidov, and I. V. Smolyar (2018a), An inventory of Arctic Ocean data in the World Ocean Database, *Earth Syst. Sci. Data*, *10*(1), 677-687, doi:10.5194/essd-10-677-2018.

Zweng, M. M.*, and Co-authors* (2018b), World Ocean Atlas 2018, Volume 2: Salinity (A. Mishonov Technical Ed.); NOAA Atlas NESDIS 82, 50 pp.*Rep.*, 50 pp, NOAA/NESDIS, Silver Spring, MD.